Electronic structure of strongly correlated materials
Part II

Vladimir I. Anisimov

Institute of Metal Physics
Ekaterinburg, Russia

LDA+U method applications

- **Mott insulators**
- **Charge order: Fe_3O_4**
- **Spin order: calculation of exchange interaction parameters in CaV_nO_{2n+1}**
- **Orbital order: $KCuF_3$, $LaMnO_3$**
- **Charge and orbital order: $Pr_{0.5}Ca_{0.5}MnO_3$**
- **Low-spin to high-spin transition: Co^{+3} in $LaCoO_3$**
- **Stripe phase of cuprates**

LDA+U method applications

Mott insulators that are small gap semiconductors
or even metals in LSDA are correctly reproduced in LDA+U
as wide gap magnetic insulators with well localized d-electrons

Table 1. Experimental (exp) and calculated (LDA + U and LSDA) spin moment (m in μ_B) and energy gap (E in eV) values of the late-3d-transition-metal oxides.

	E_{LSDA}	E_{LDA+U}	E_{exp}	m_{LSDA}	m_{LDA+U}	m_{exp}
$CaCuO_2$	0.0	2.10	1.5	0.0	0.66	0.51
CuO	0.0	1.9	1.4	0.0	0.74	0.65
NiO	0.2	3.1	4.3, 4.0	1.0	1.59	1.77, 1.64, 1.90
CoO	0.0	3.2	2.4	2.3	2.63	3.35, 3.8
FeO	0.0	3.2	2.4	3.4	3.62	3.32
MnO	0.8	3.5	3.6–3.8	4.61	1.67	4.79, 4.58

V.Anisimov et al, Phys.Rev. B 44, 943 (1991)

LDA+U method applications

The density of states for ferromagnetic Gd metal from LDA+*U* calculation and results of BIS (bremsstrahlung isochromat spectroscopy) and XPS (x-ray photoemission spectroscopy) experiments.

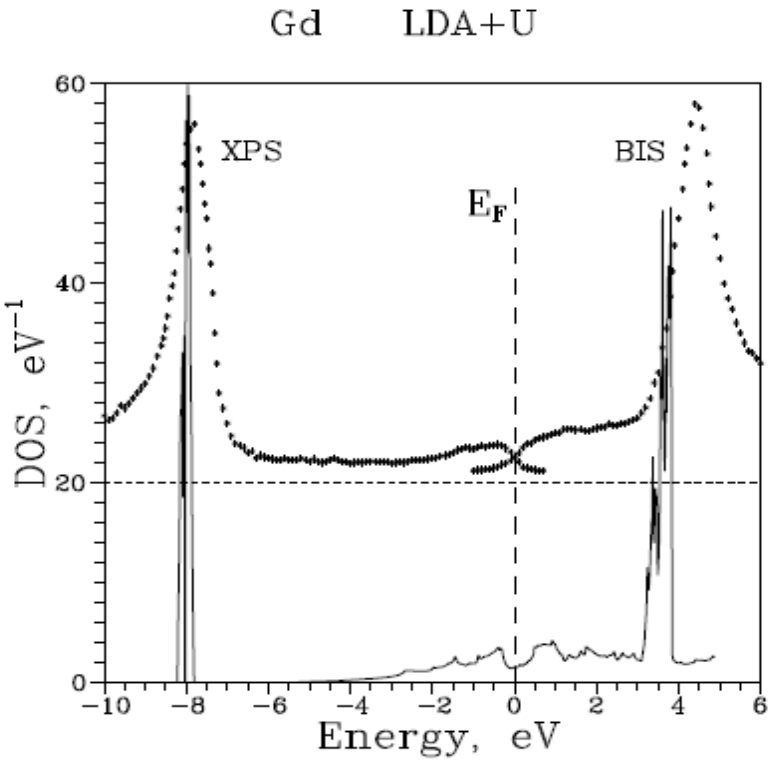

Antiferromagnetic Mott insulator $CaCuO_2$ (in LDA nonmagnetic metal)

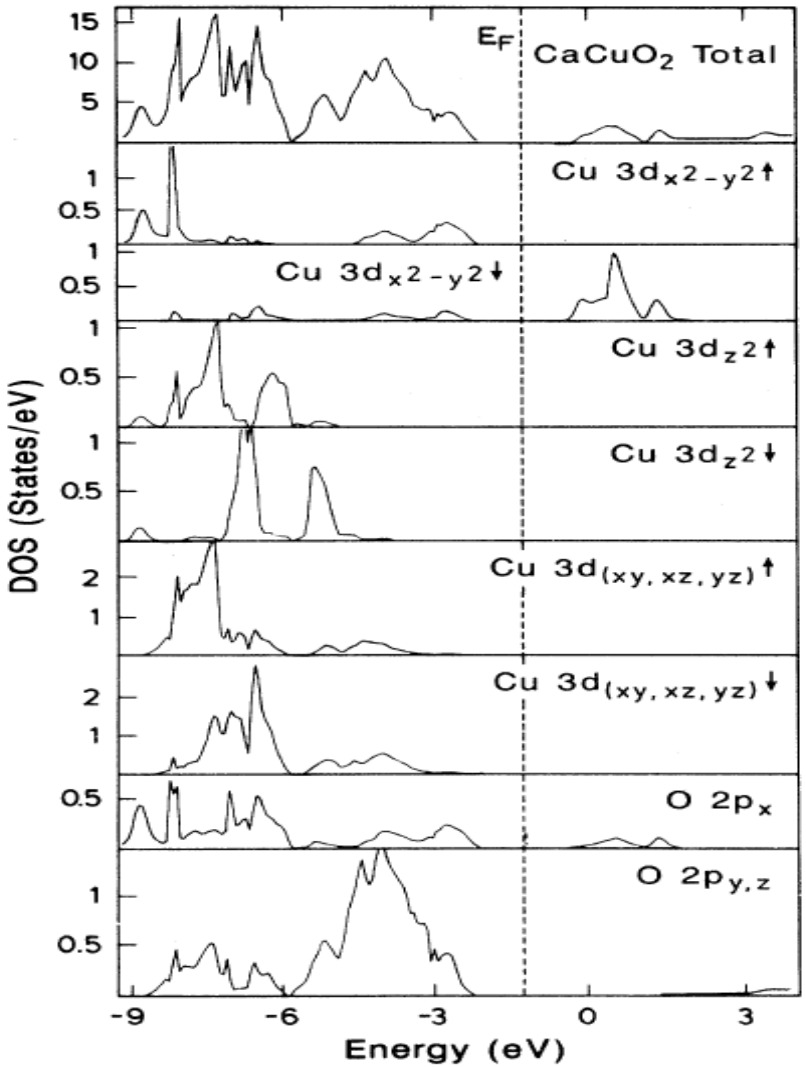

Charge order in Fe_3O_4

Fe_3O_4 has spinel crystal structure

one Fe^{+3} ion in tetrahedral position (A)

two $Fe^{+2.5}$ ions in octahedral positions (B)

Below T_V=122K a charge ordering happens ← **Verwey transition**

Simultaneous metal-insulator transition:

half of the octahedral positions is occupied by Fe^{+3} and other half by Fe^{+2}.

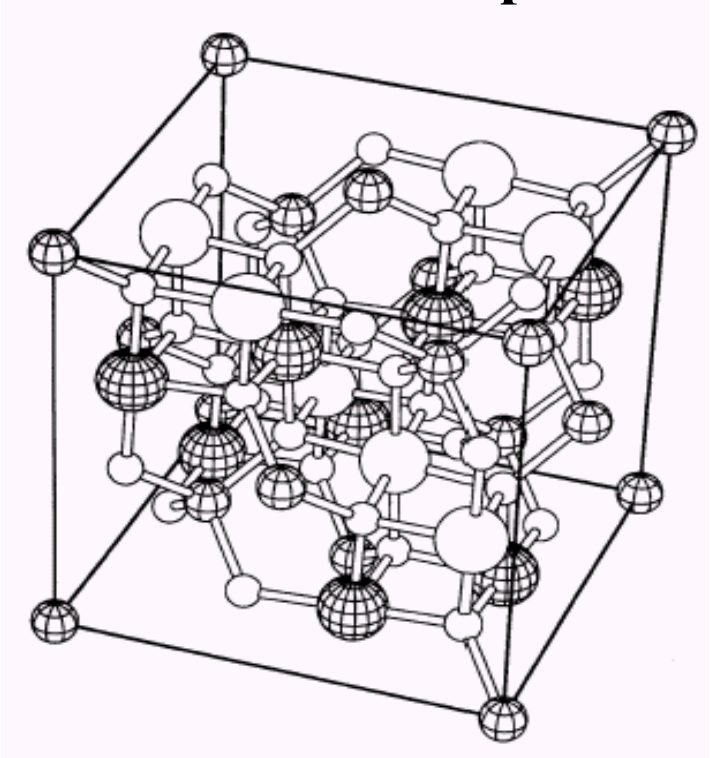

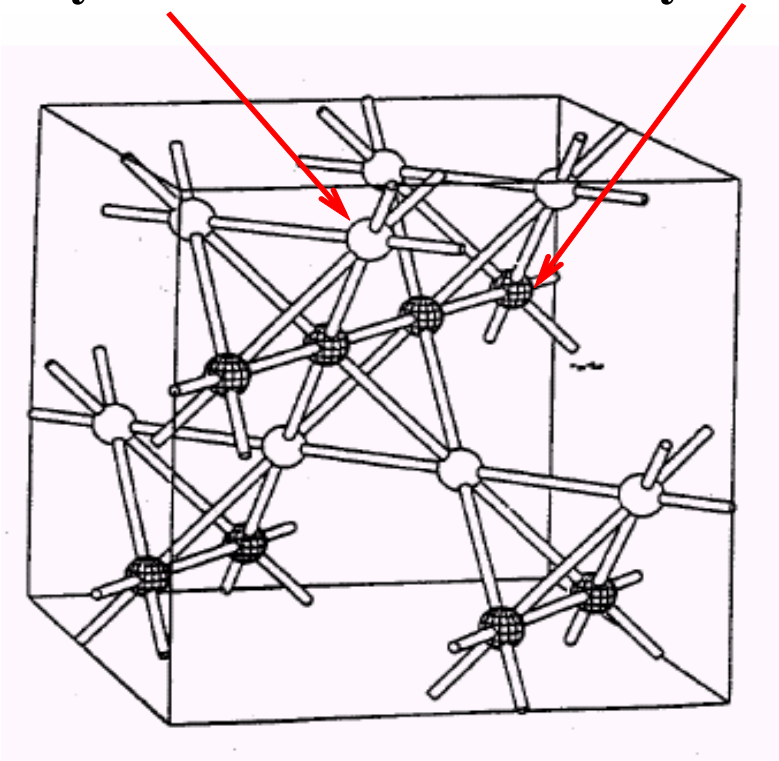

V.Anisimov et al, Phys. Rev.B 54, 4387 (1996)

LDA and charge order problem

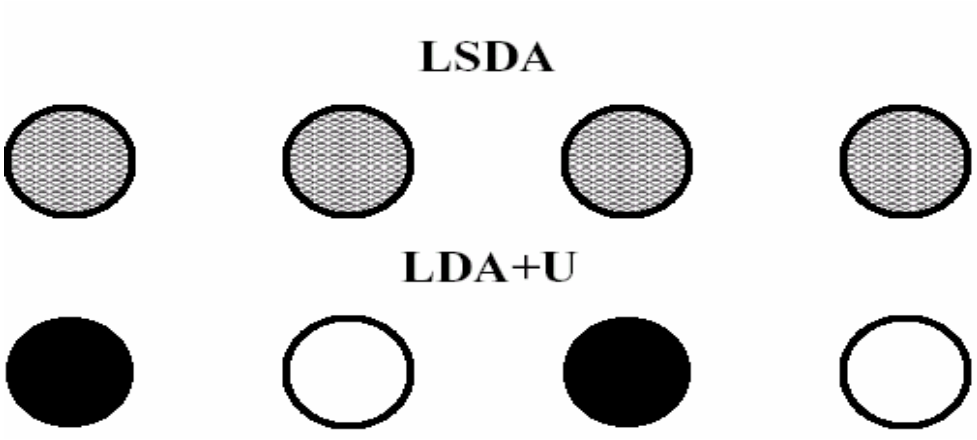

Charge disproportionation in LSDA is unstable due to self-interaction problem

$$U = \frac{d\varepsilon}{dn}; \qquad \varepsilon_1^{LSDA}(n_0 - \delta n) = \varepsilon_0 - U\delta n; \quad \varepsilon_2^{LSDA}(n_0 + \delta n) = \varepsilon_0 + U\delta n;$$

in LDA+U self-interaction is explicitly canceled

$$\varepsilon_1 = \varepsilon_1^{LSDA}(n_0 - \delta n) + U\left(\frac{1}{2} - (n_0 - \delta n)\right) = \varepsilon_0 - U\left(\frac{1}{2} - n_0\right)$$

$$\varepsilon_2 = \varepsilon_2^{LSDA}(n_0 + \delta n) + U\left(\frac{1}{2} - (n_0 + \delta n)\right) = \varepsilon_0 - U\left(\frac{1}{2} - n_0\right)$$

LSDA and LDA+U results for Fe_3O_4

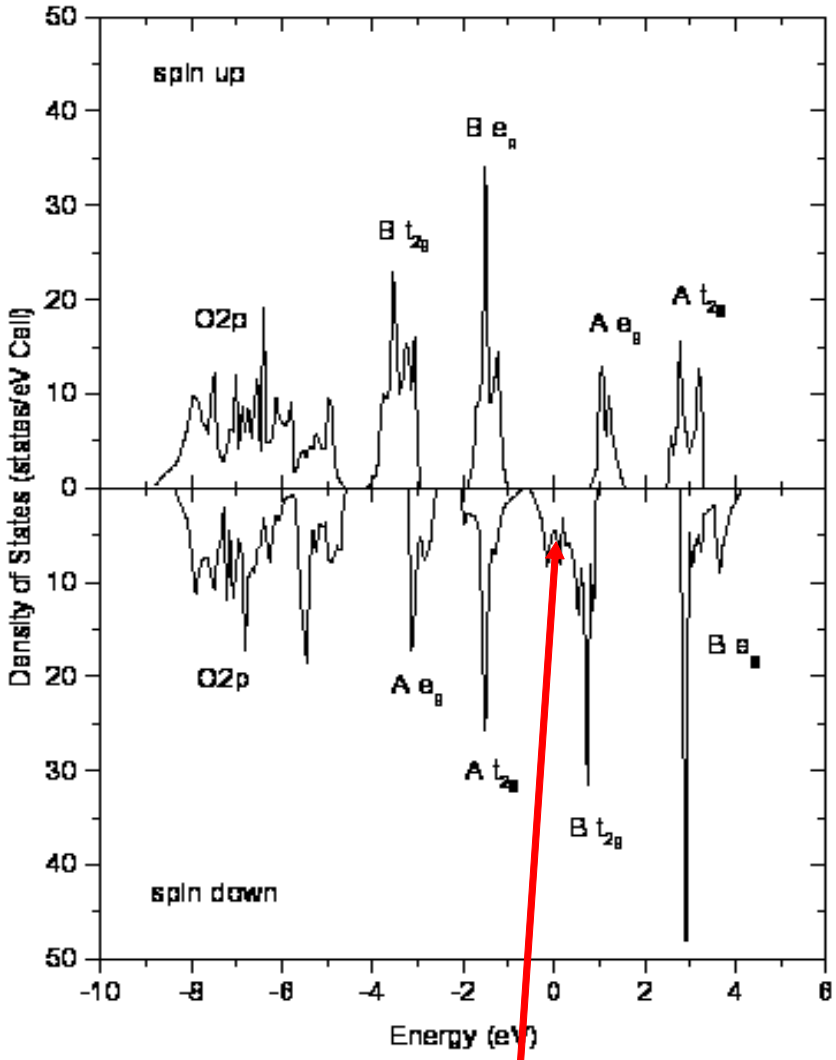

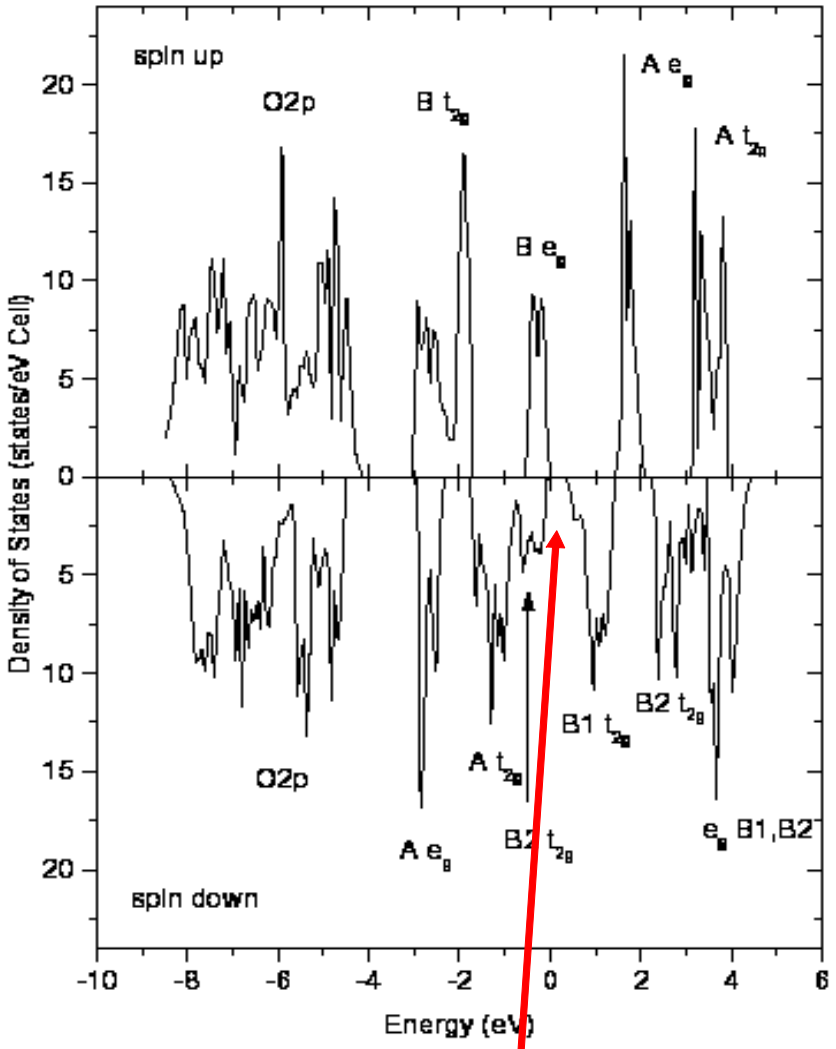

metal

insulator

Fe_3O_4

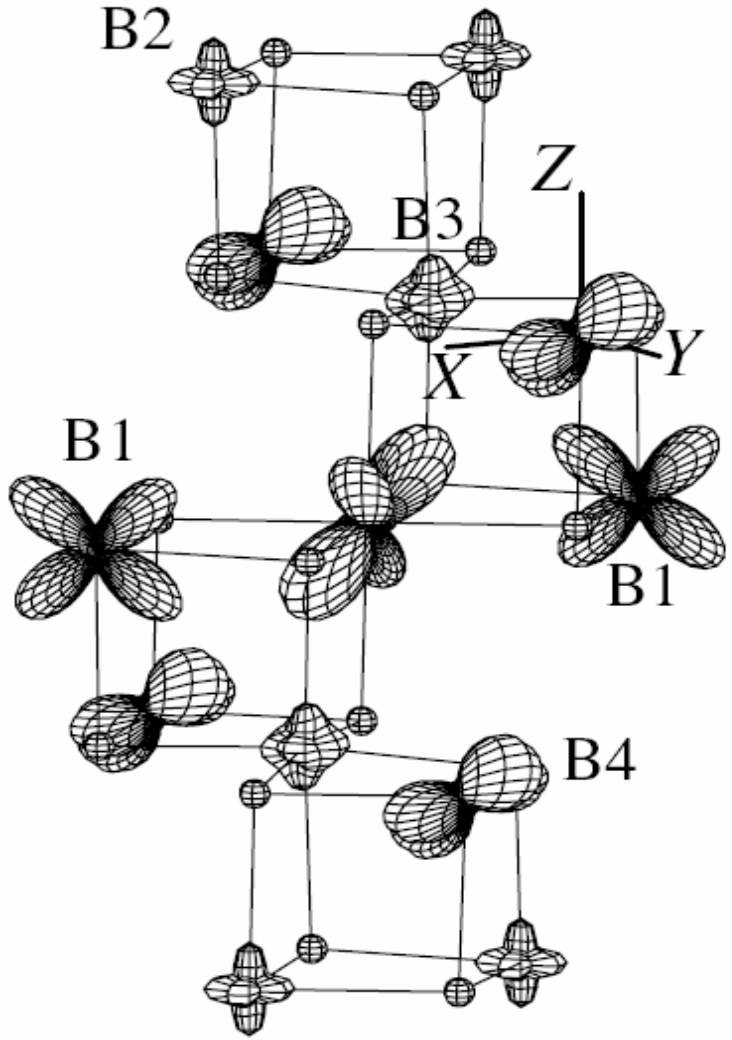

Charge and orbital order in experimental low-temperature monoclinic crystal structure Fe_3O_4

I.Leonov et al,
PRL93,146404 (2004)

Charge and orbital order in experimental low-temperature monoclinic crystal structure Fe_3O_4

TABLE I. Total and l-projected charges, magnetic moments, and occupation of the most populated t_{2g} minority orbitals calculated for inequivalent Fe_B ions in the low-temperature $P2/c$ phase of Fe_3O_4 [28].

Fe_B ion	q	q_s	q_p	q_d	M (μ_B)	$t_{2g\downarrow}$ orbital	n
Fe_{B1}	6.04	0.17	0.19	5.69	3.50	$d_{xz} \mp d_{yz}$	0.76
Fe_{B2}	5.73	0.19	0.21	5.44	3.94		0.09
Fe_{B3}	5.91	0.19	0.21	5.51	3.81		0.09
Fe_{B4}	6.03	0.16	0.18	5.69	3.48	$d_{x^2-y^2}$	0.80

Exchange interactions in layered vanadates

CaV_nO_{2n+1} (n=2,3,4) systems show a large variety of magnetic properties:

- **n=3: CaV_3O_7 has unusual long-range spin order**
- **n=4: CaV_4O_9 is a frustrated (plaquets) system with a spin gap value 107K**
- **n=2: CaV_2O_5 is a set of weakly coupled dimers with a large spin gap 616 K**
- **isostructural MgV_2O_5 has very small spin gap value < 10K**

Fully ab-initio description of magnetic properties

LDA+U calculations: eigenfunctions and eigenvalues → Exchange couplings calculations using LDA+U results → Heisenberg model is solved by QMC

V.Anisimov et al, Phys.Rev.Lett. 83, 1387 (1999)

Crystal structure and orbitals

Crystal structure of CaV_nO_{2n+1} **is formed by VO_5 pyramids connected into layers.**

V^{+4} ions in d^1 configuration.

The occupied d_{xy}-orbital of V^{+4} ions in CaV_3O_7

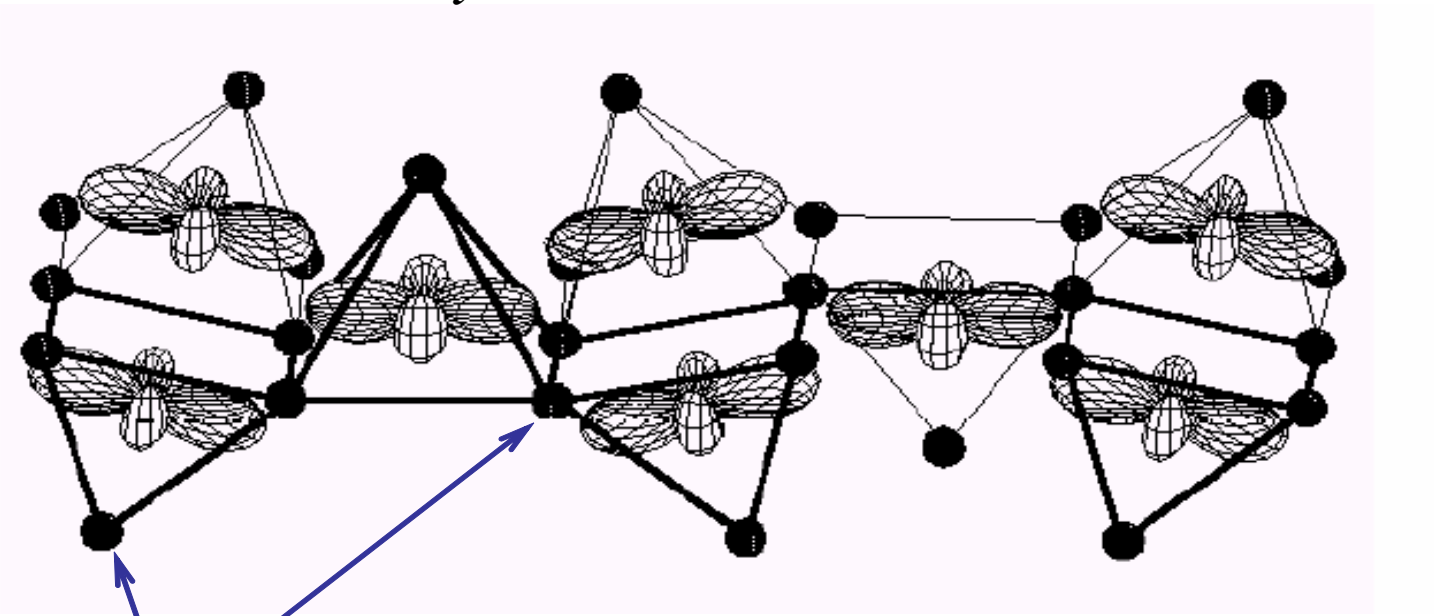

Oxygen atoms form pyramids with V atoms inside them.

Exchange couplings scheme

The basic crystal structure and the notation of exchange couplings in

CaV_2O_5 and MgV_2O_5 **CaV_3O_7** **CaV_4O_9**

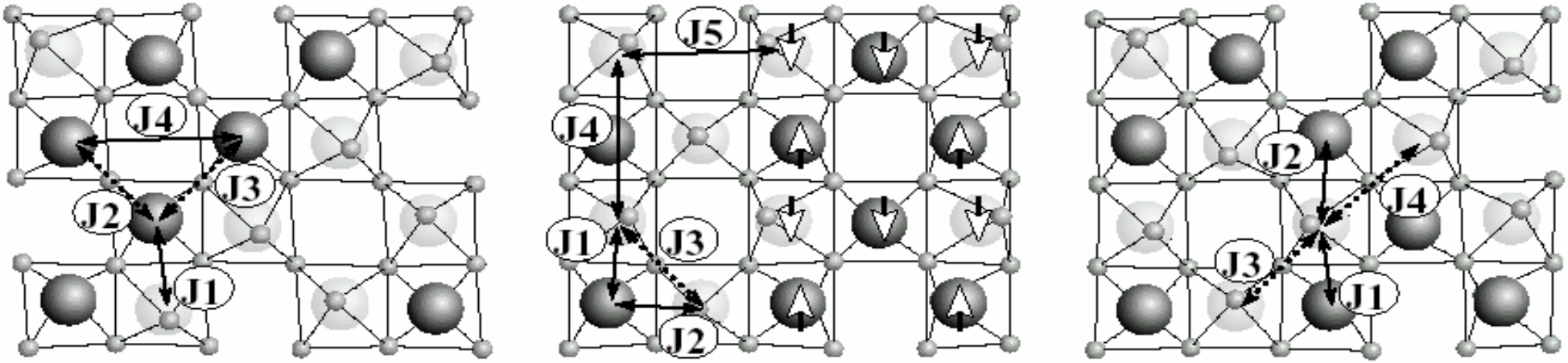

V atoms represented by large circles with different colors have different z-coordinate

Oxygen atoms are shown by small circles

Long range magnetic structure of CaV_3O_7 is depicted by white arrows

	CaV_2O_5	MgV_2O_5	CaV_3O_7	CaV_4O_9
*J*1	–28	60	46	62
*J*2	608	92	–14	89
*J*3	122	144	75	148
*J*4	20	19	18	91

QMC solution of Heisenberg model

Comparison of the calculated and measured susceptibility

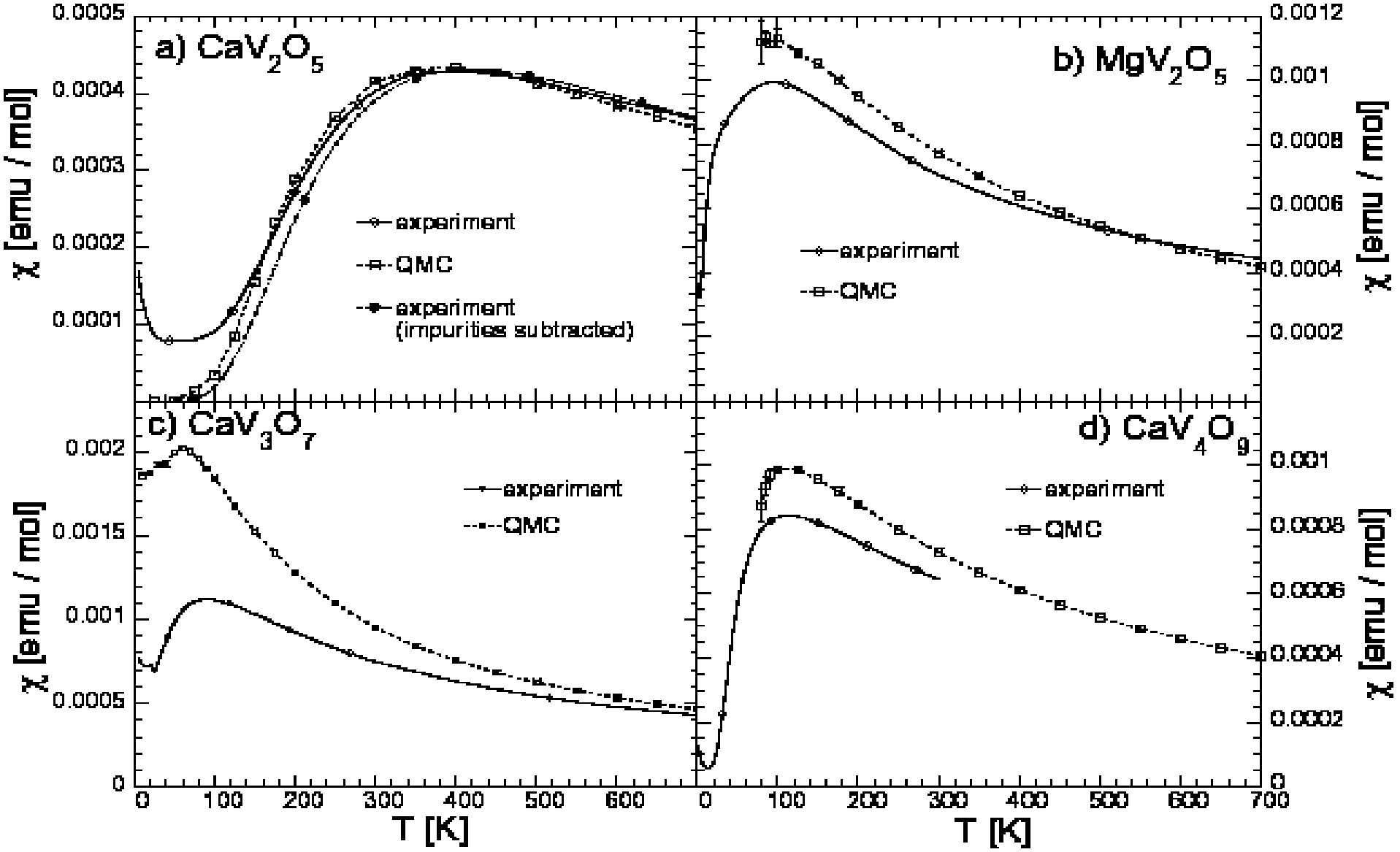

Orbital order in $KCuF_3$

$KCuF_3$ has cubic perovskite crystal structure

with Jahn-Teller distorted CuF_6 octahedra.

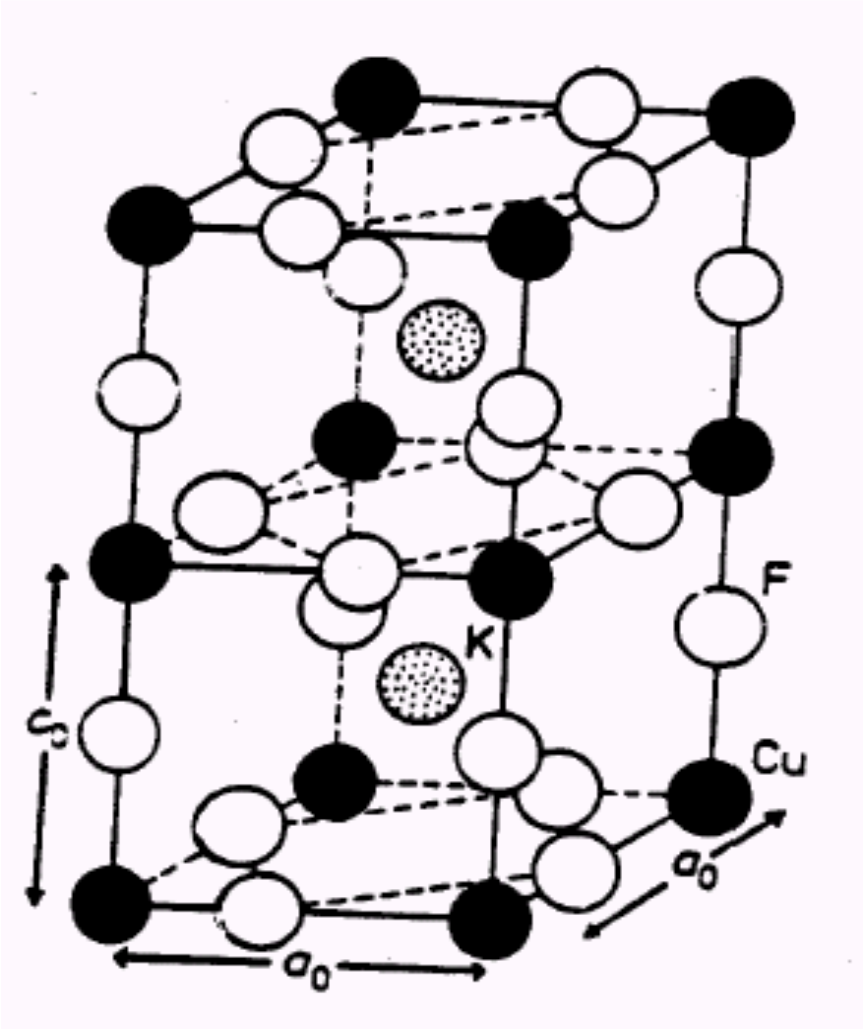

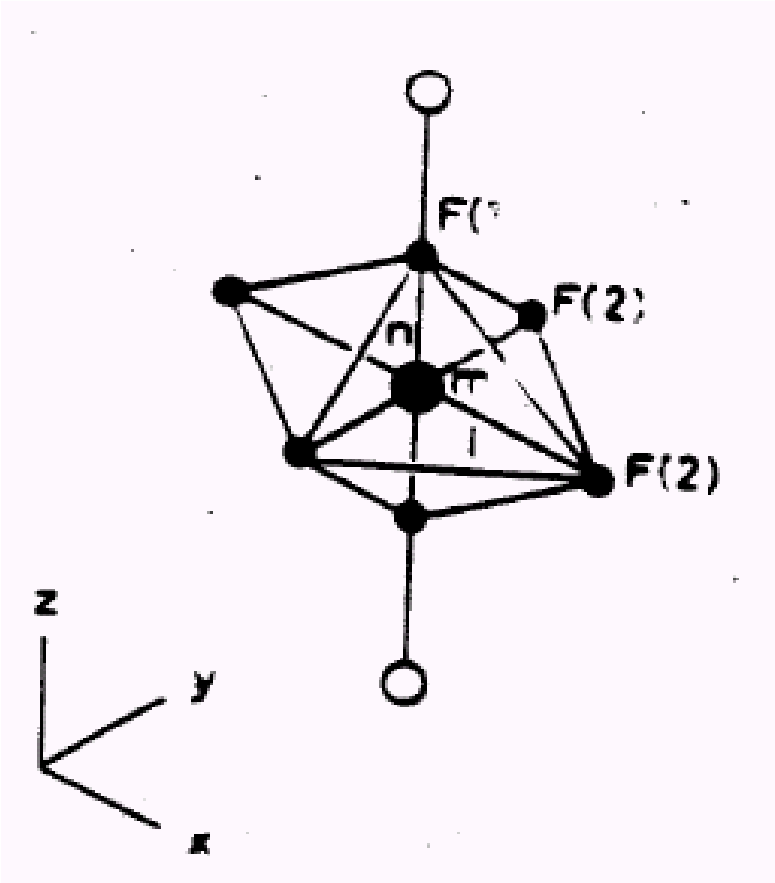

Orbital order in $KCuF_3$

In $KCuF_3$ Cu^{+2} ion has d^9 configuration **with a single hole in e_g doubly degenerate subshell.**

Experimental crystal structure

antiferro-orbital order

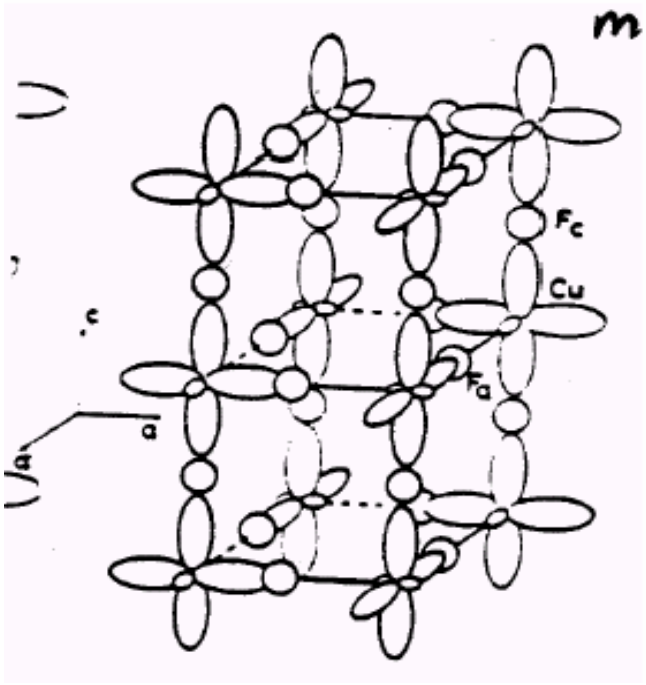

LDA+U calculations for *undistorted* perovskite structure

hole density of the same symmetry

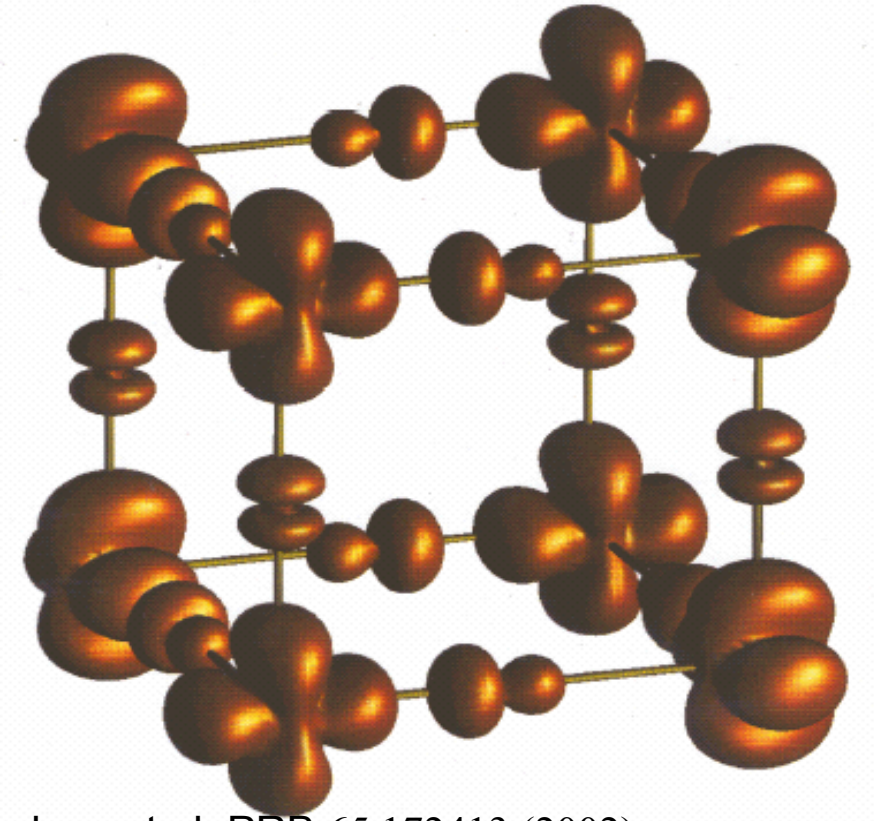

A.Lichtenstein et al, Phys. Rev.B **52,** R5467 (1995); J.Medvedeva et al, PRB 65,172413 (2002)

Cooperative Jahn-Teller distortions in $KCuF_3$

LSDA gave cubic perovskite crystal structure stable in respect to Jahn-Teller distortion of CuF_6 octahedra

Only LDA+U produces total energy minimum for distorted structure

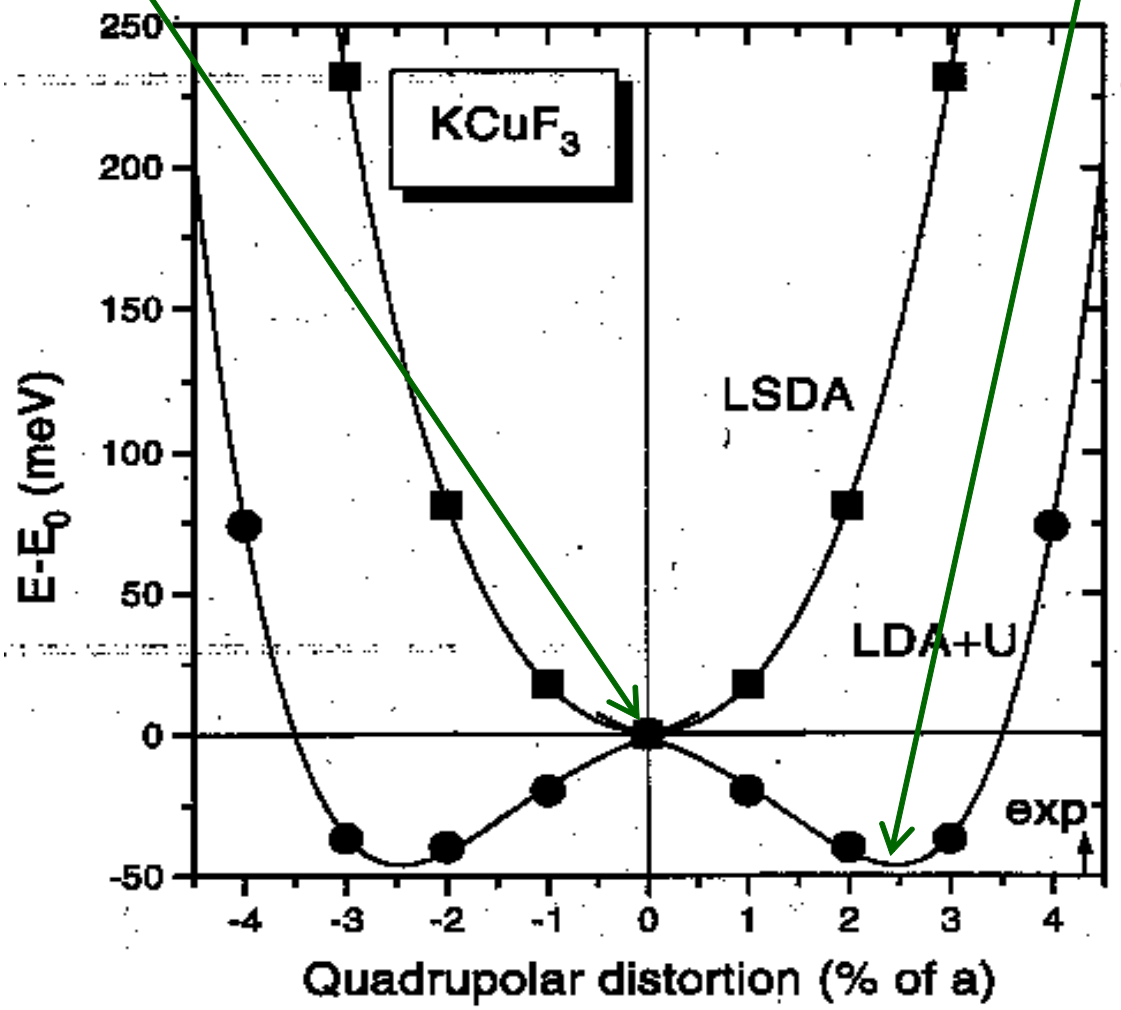

Calculated exchange couplings:
c-axis 17.5 meV
ab-plane –0.2 meV
One-dimensional antiferromagnet

Orbital order in $Pr_{1-x}Ca_xMnO_3$ (x=0 and 0.5)

$PrMnO_3$ has orthorhombic perovskite crystal structure

with tilted and rotated Jahn-Teller distorted MnO_6 octahedra.

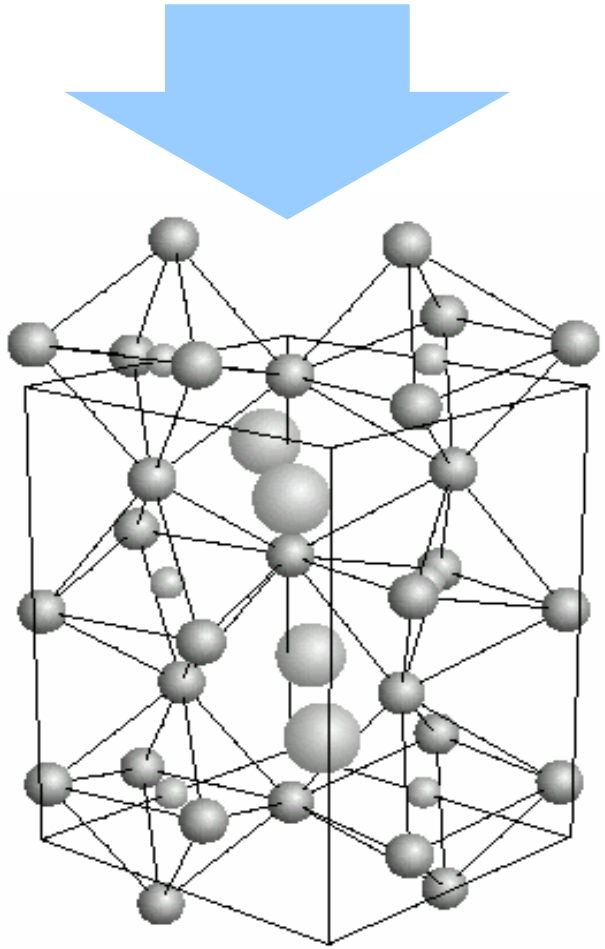

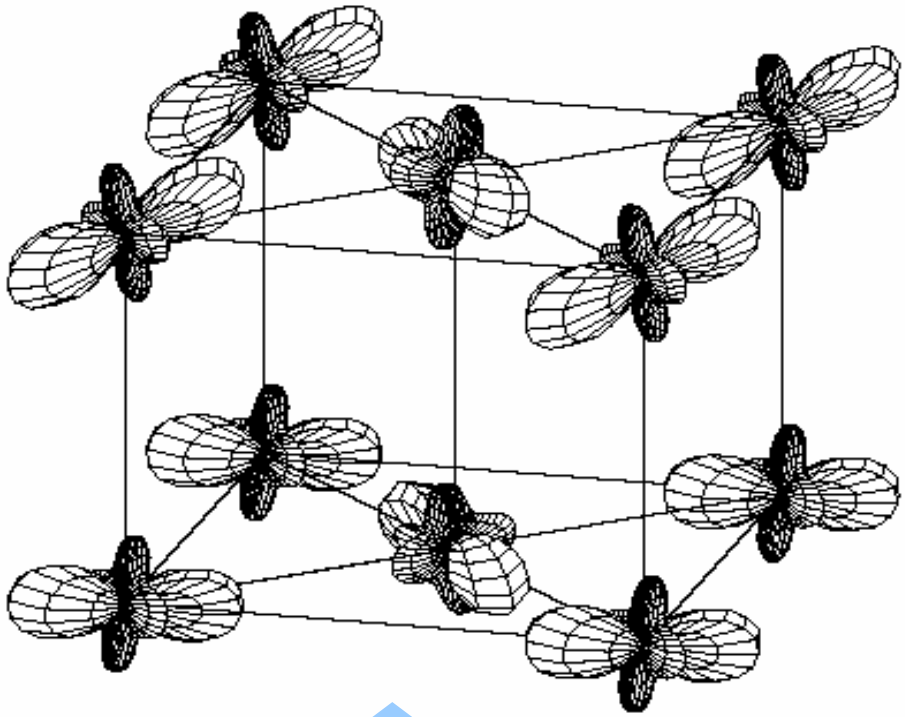

Orbital order for partially filled e_g shell of Mn^{+3} ion in $PrMnO_3$ in a crystal structure *without* JT-distortion from LDA+U

$Pr_{0.5}Ca_{0.5}MnO_3$

experimental magnetic and charge-orbital order

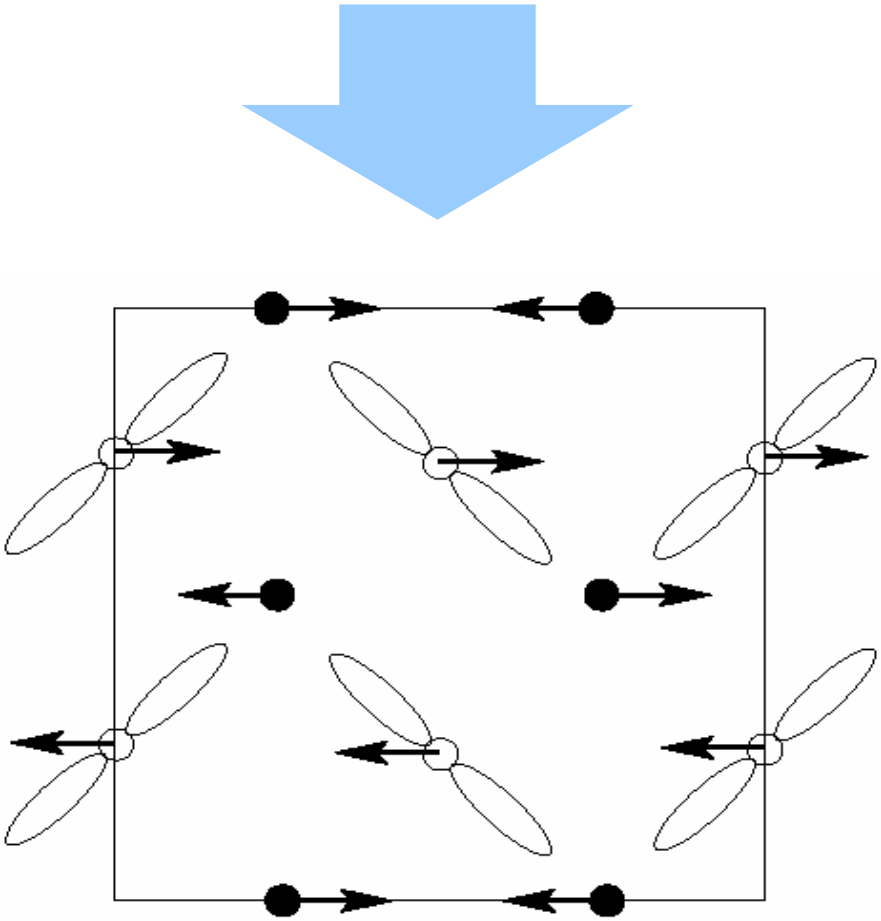

Orbital order for partially filled e_g shell of Mn^{+3} ion in $Pr_{0.5}Mn_{0.5}O_3$ in a crystal structure *without* JT-distortion from LDA+U

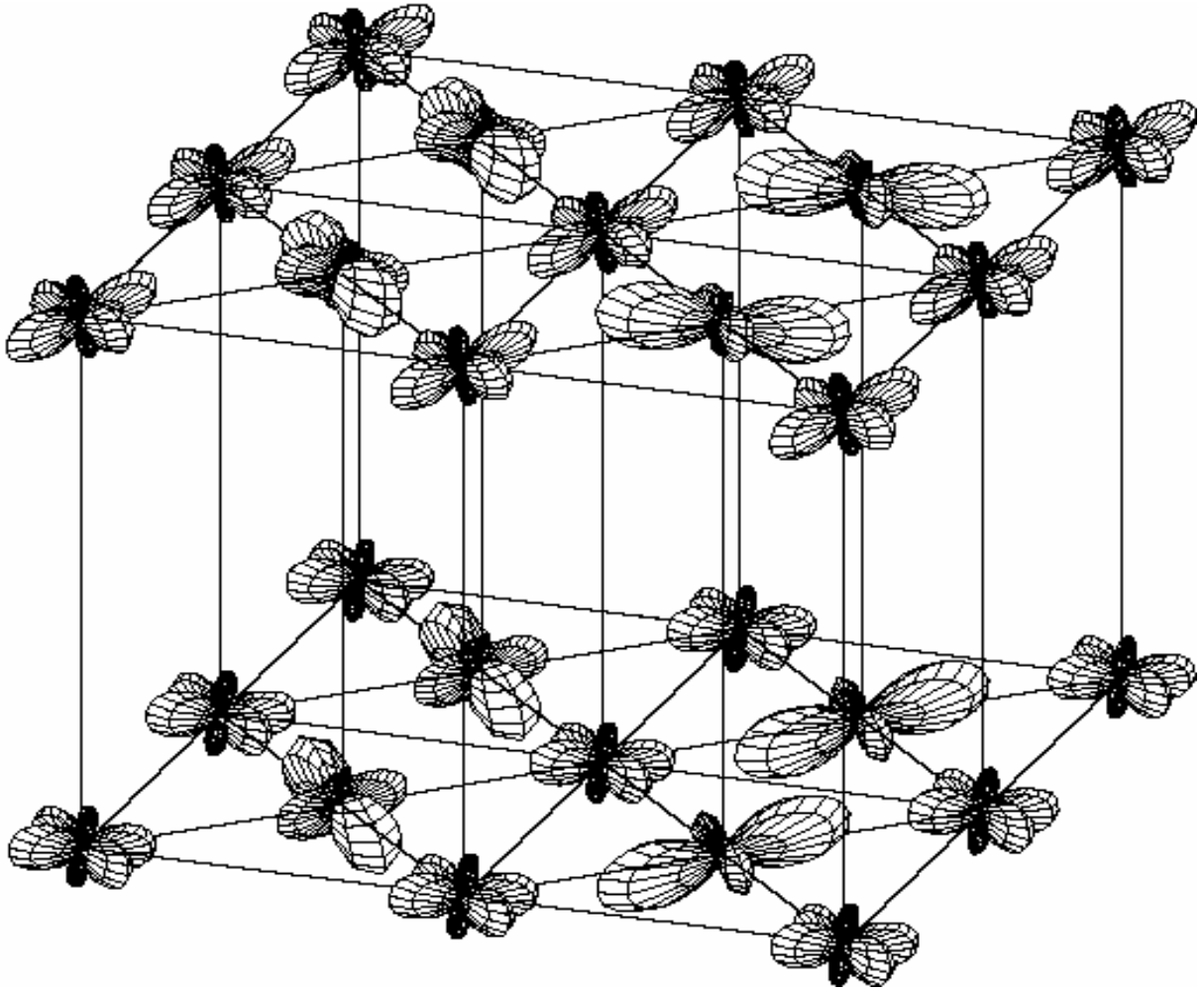

V.Anisimov et al, Phys.Rev.B **55**, 15 494 (1997); M.Korotin, PRB62, 5696 (2000)

Spin state of Co^{+3} in $LaCoO_3$

3d-level scheme for low-spin ground state

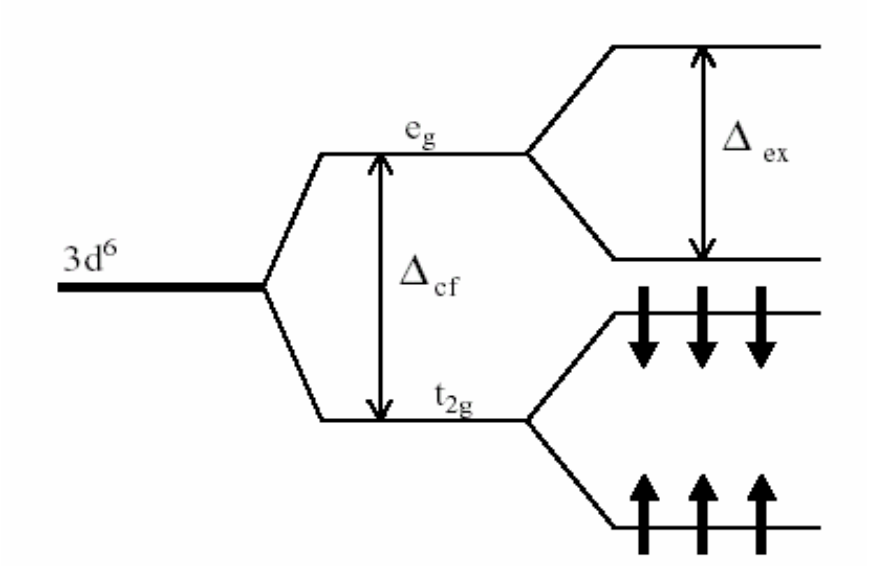

Scheme representation of various Co d^6+d^7L configurations in different spin states:

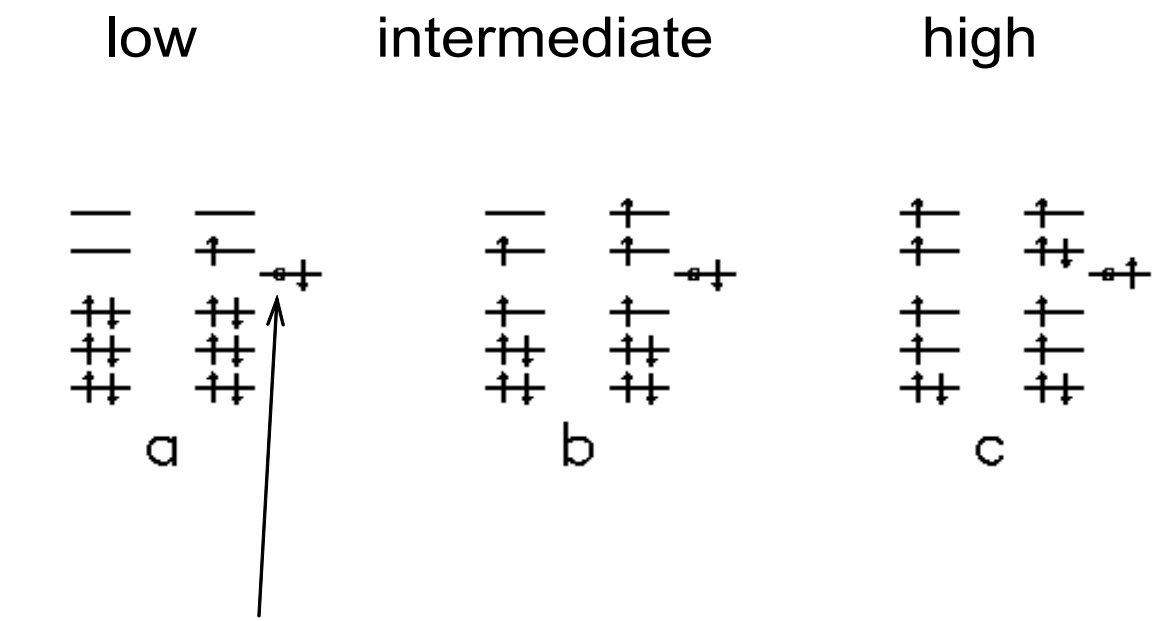

M.Korotin et al, Phys.Rev.B **54** (1996) 5309; I.Nekrasov et al, Phys. Rev. B **68**, 235113 (2003)

Spin state of Co^{+3} in $LaCoO_3$

The total energies for various spin states of $LaCoO_3$

relative to the energy of $t_{2g}^6 e_g^0$ state versus R3c lattice constant.

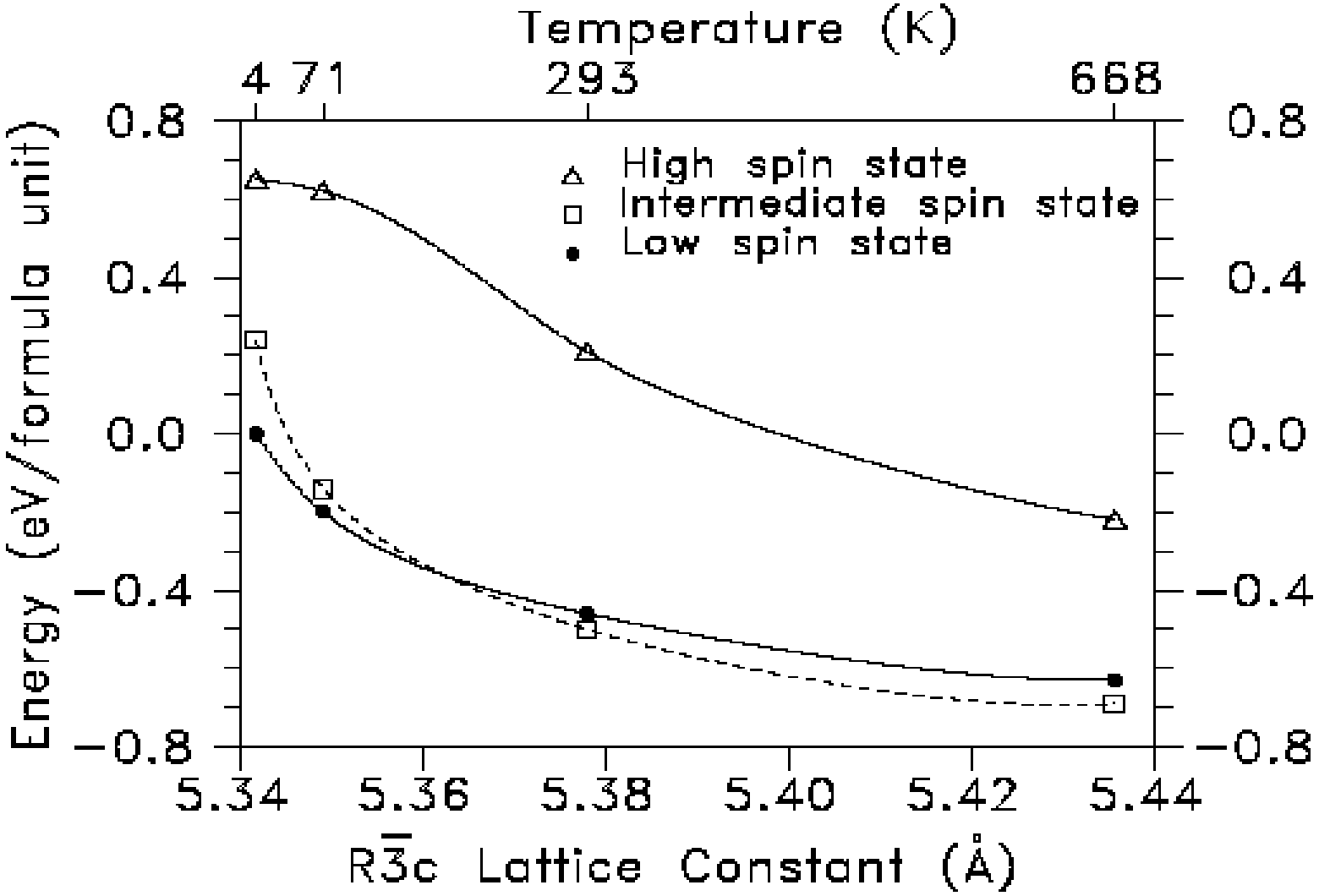

$HoCoO_3$ versus $LaCoO_3$

The rhombohedral crystal structure of $LaCoO_3$ (left) and the orthorhombic crystal structure of $HoCoO_3$ (right). Co - large spheres; O - small spheres.

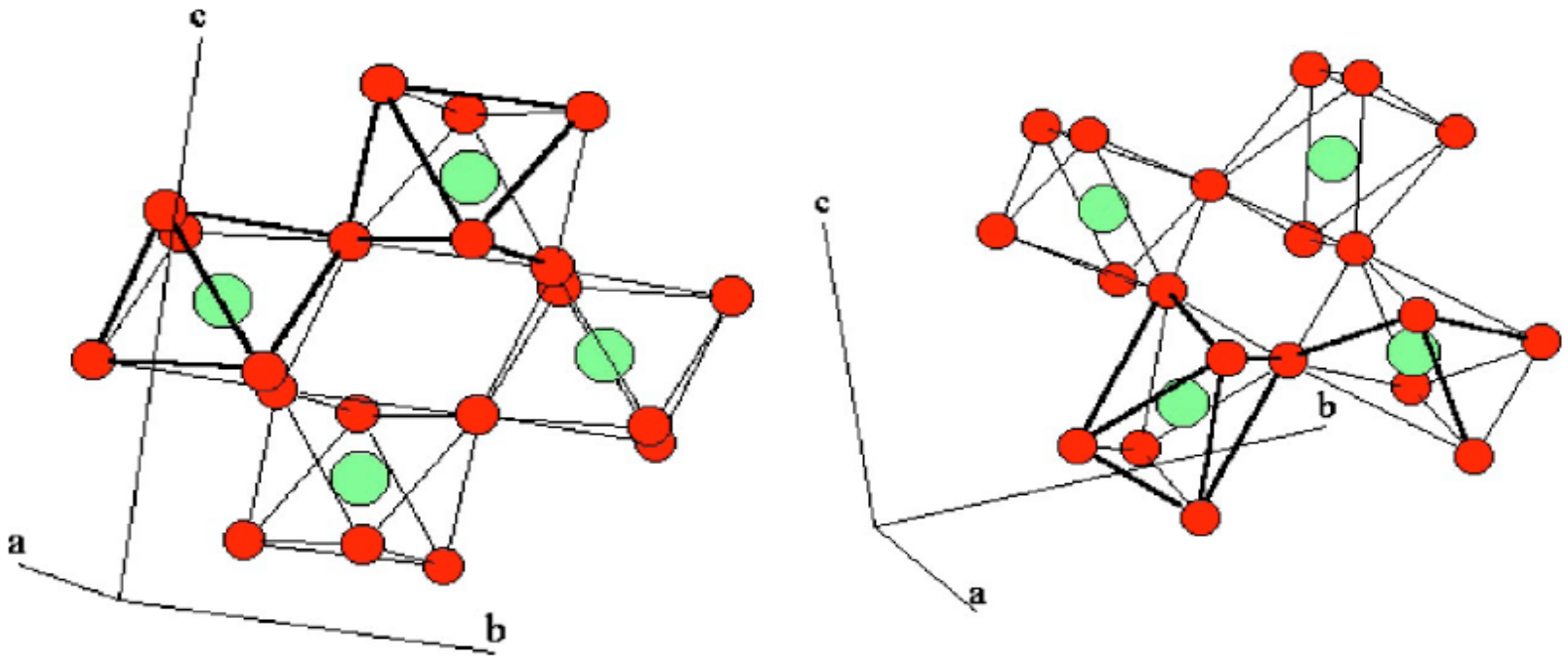

$HoCoO_3$ versus $LaCoO_3$

Comparison of total energy per Co ion of intermediate and low-spin state solutions for $LaCoO_3$ and $HoCoO_3$ calculated with the LDA+U approach as a functions of temperature. The temperature of transition is calculated as the temperature where two lines cross.

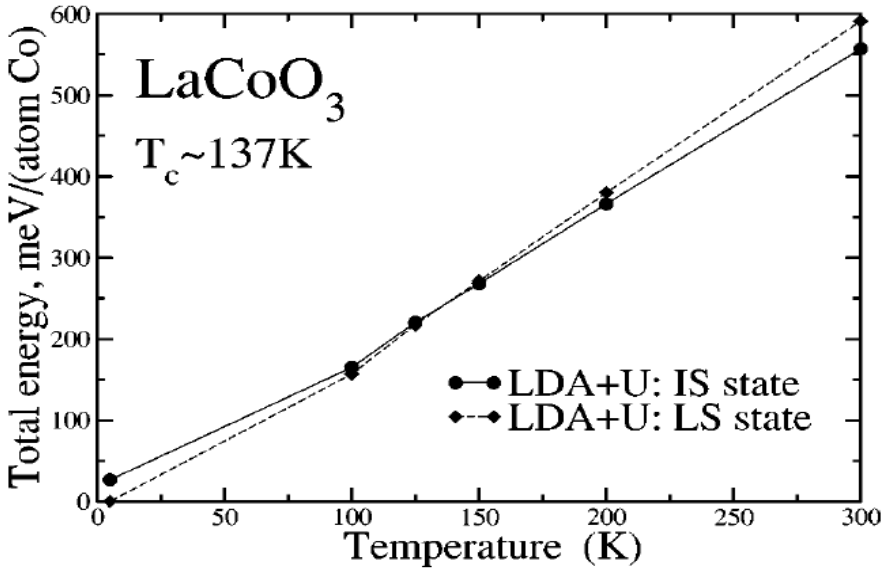

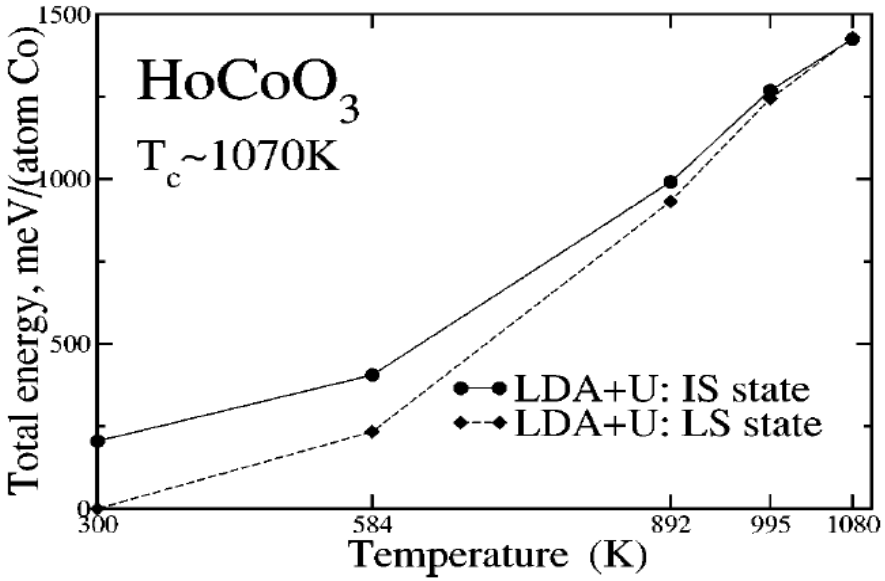

I. A. Nekrasov *et al*, PRB 68, 235113 (2003)

Stripe phase in cuprates ($La_{7/8}Sr_{1/8}CuO_4$)

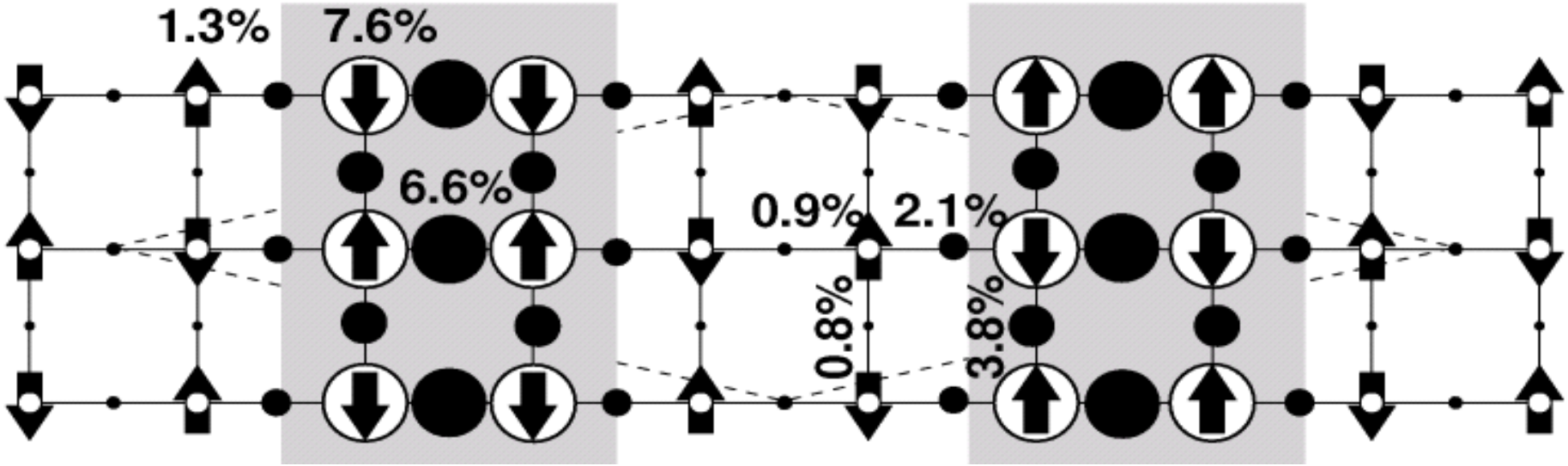

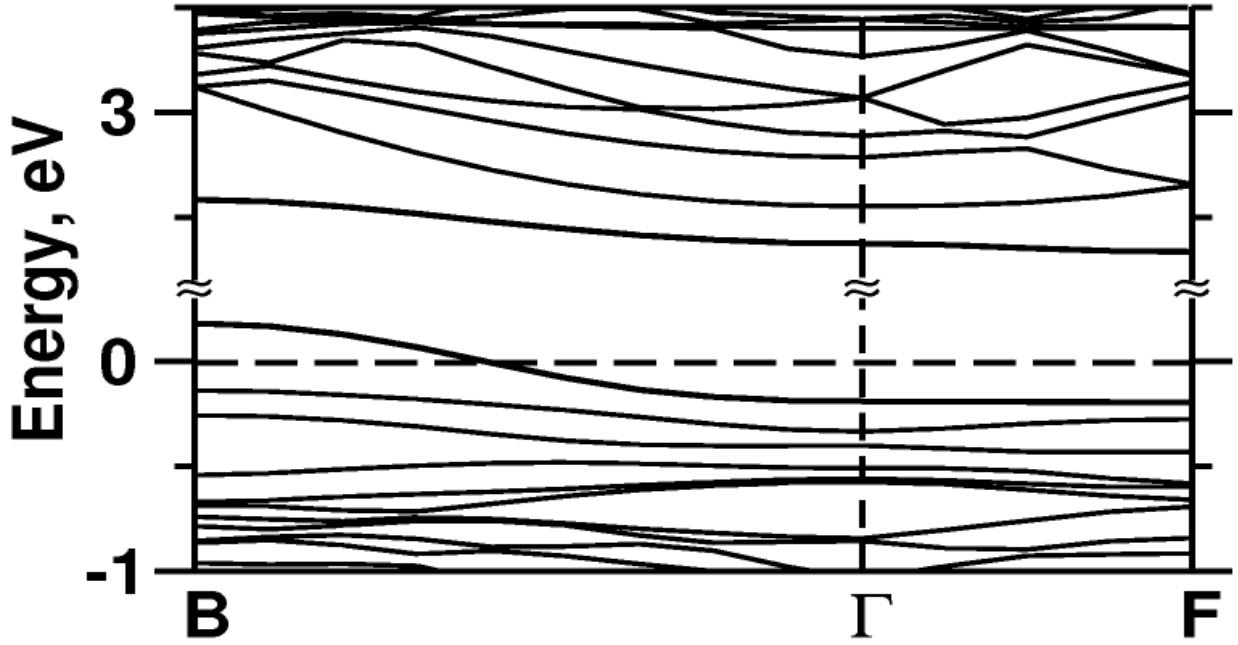

V.Anisimov et al, Phys. Rev. B 70, 172501 (2004)

Wannier function for metallic stripe band

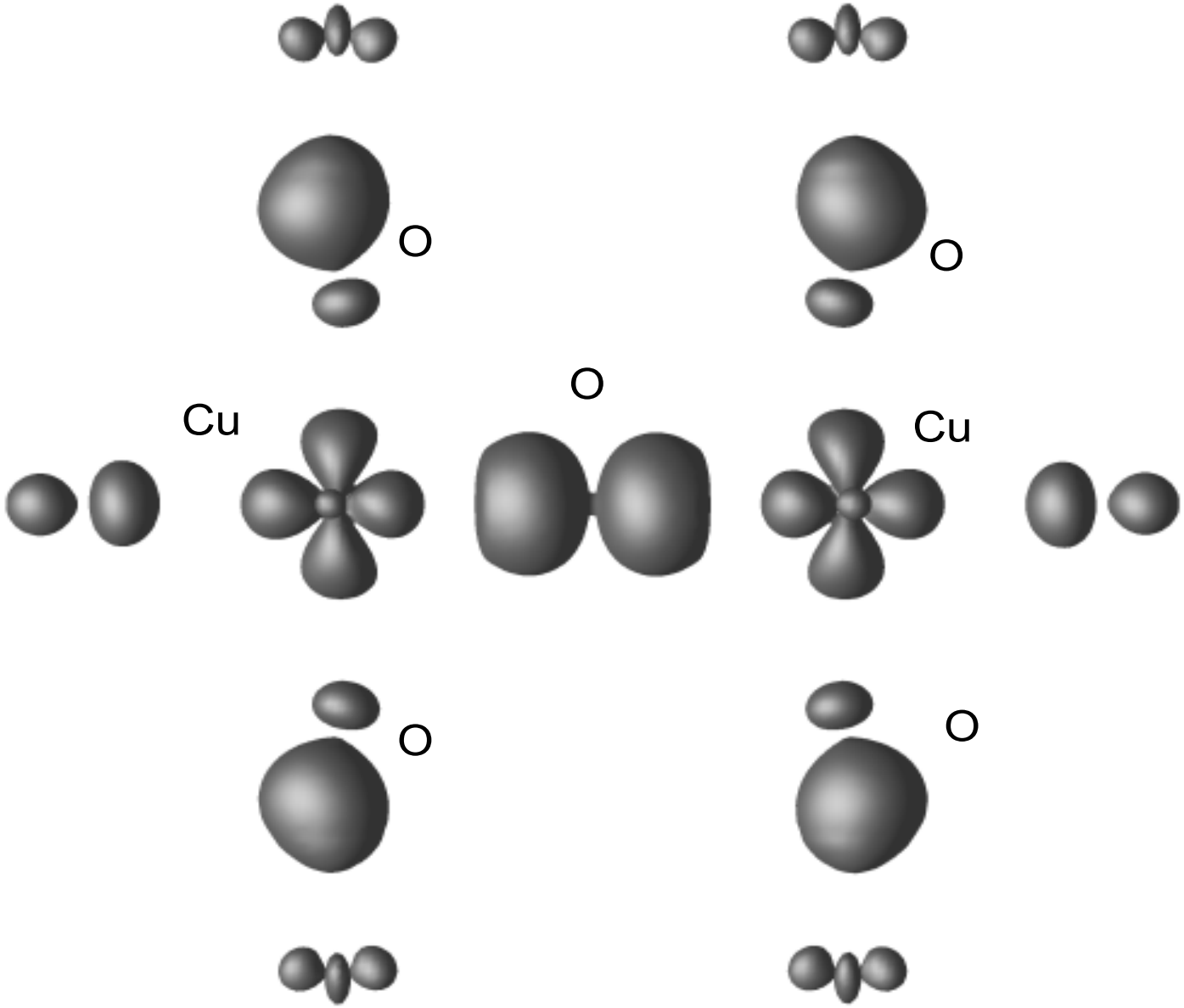

Exchange couplings for AF domain

Two-leg ladder

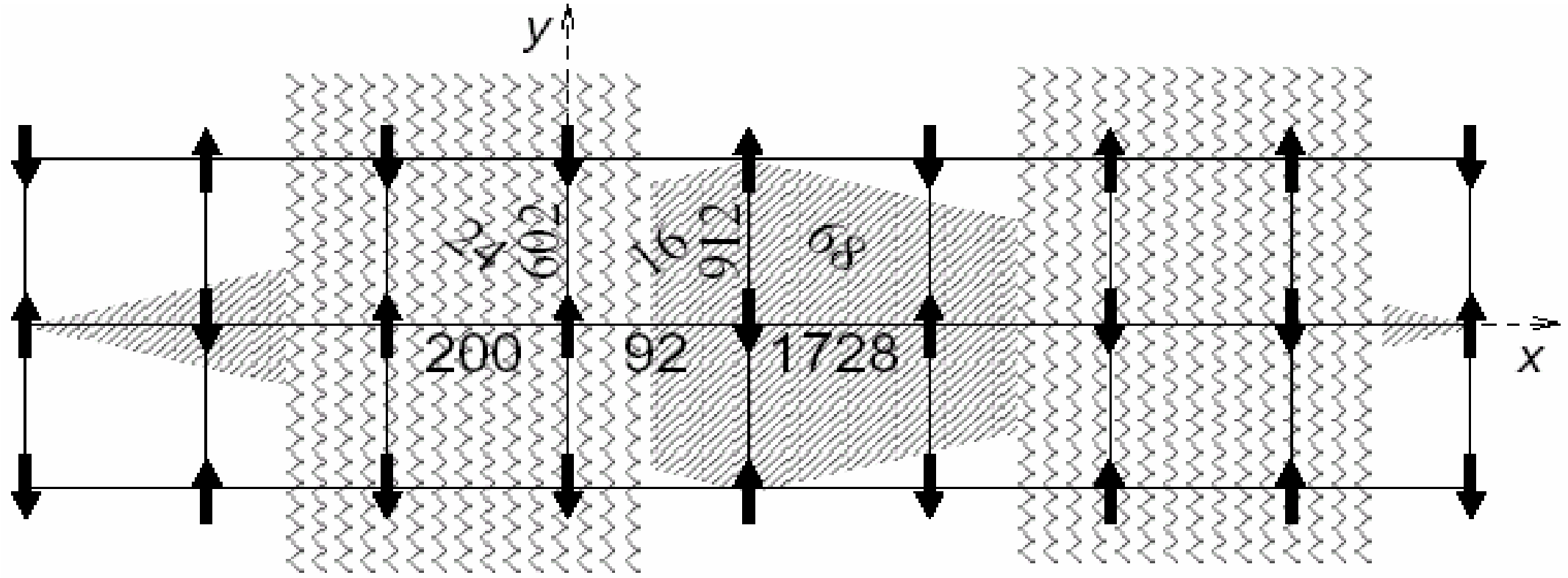

Other LDA+U results

- **Magnetic transition in $FeSi_{1-x}Ge_x$**
  (PRL 76 (1996) 1735; PRL 89, 257203 (2002)
- **Exchange couplings in molecular magnet Mn-12 ($[Mn_{12}O_{12}(CH_3COO)_{16}(H_2O)_4]2CH_3COOH4H_2O$)**
  (PRB 65, 184435 (2002))
- **Insulating ground state of quarter-filled ladder NaV_2O_5 (PRB 66, 081104 (2002))**
- **CrO_2 : a self-doped double exchange ferromagnet**
  (PRL 80, 4305 (1998))
- **Mott-Hubbard insulator on Si-terminated SiC(0001) surface (PRB 61, 1752 (2000))**
- **Polaron effects in $La_{2-x}Sr_xCuO_4$ and $La_{2-x}Sr_xNiO_4$**
  (PRL 68, 345 (1992);PRB 55,12829 (1997); PRB 66, 100502 (2002))
- **Antiferromagnetism in linear-chain Ni compound $[Ni(C_6H_{14}N_2)_2]$ $[Ni(C_6H_{14}N_2)_2Cl_2]Cl_4$ (PRB 52,6975 (1995))**

LDA+DMFT

LDA+U
Static mean-field approximation
Energy-independent potential

$$\hat{V} = \sum_{mm'\sigma} | inlm\sigma > V^{\sigma}_{mm'} < inlm'\sigma |$$

LDA+DMFT
Dynamic mean-field approximation
Energy-dependent complex
self-energy operator

$$\hat{\Sigma}(\varepsilon) = \sum_{mm'\sigma} | inlm\sigma > \Sigma(\varepsilon)^{\sigma}_{mm'} < inlm'\sigma |$$

Applications:
Insulators with long-range
spin-,orbital- and charge order

Applications:
Paramagnetic, paraorbital
strongly correlated metals

Unsolved problem: short
range spin and orbital order

Dynamical cluster approximation (DCA)

Dynamical Mean-Field Theory

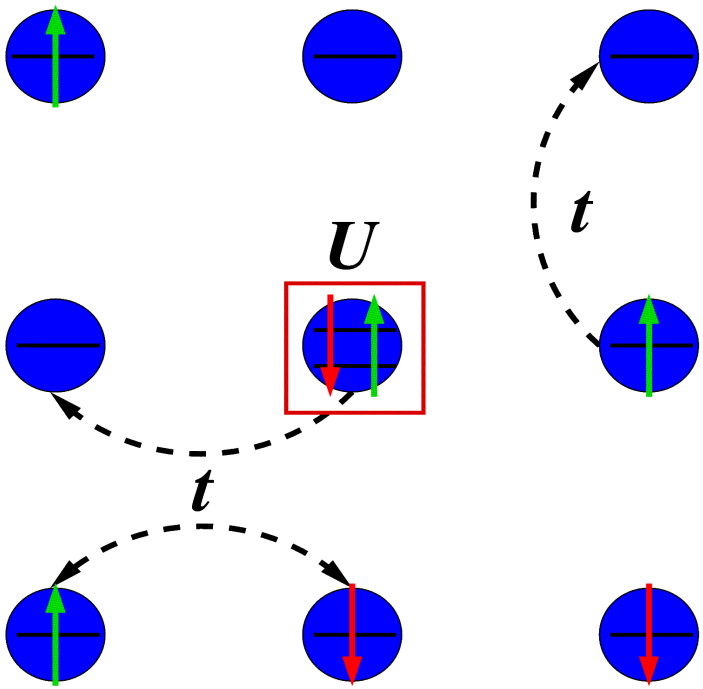

Square lattice, z=4

Object of investigation: interacting lattice fermions dynamics

Simplest description – Hubbard model

$$H = -t \sum_{<i,j>,\sigma} c_i^{\dagger} c_j + U \sum_i n_{i\uparrow} n_{j\downarrow}$$

Correlations:

$$\langle n_i n_j \rangle \neq \langle n_i \rangle \langle n_j \rangle$$

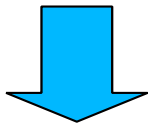

- Approximations need to be made

Dynamical Mean-Field Theory

Lattice problem is replaced by effective impurity problem with complex energy dependent potential (self-energy) on all lattice sites except distinguished one

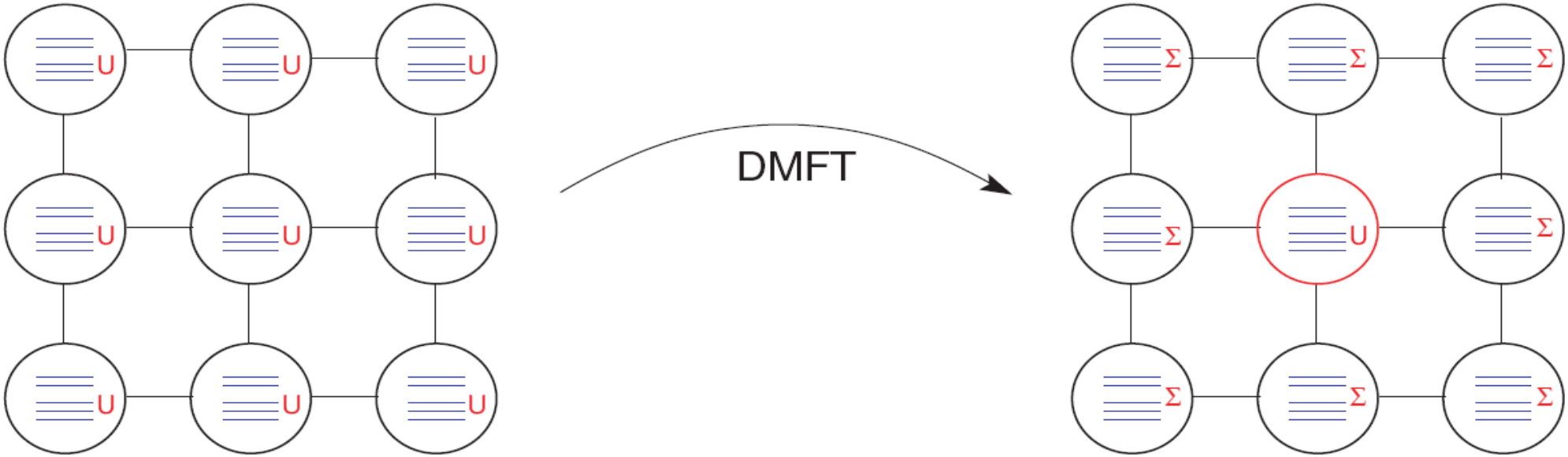

Dynamical Mean-Field Theory

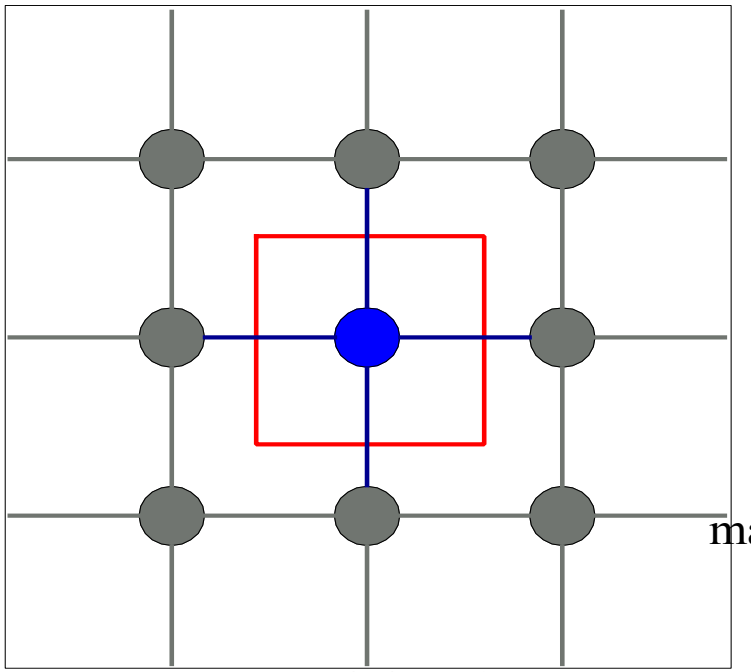

Real lattice

Mapping

Metzner, Vollhardt (1989)
$d \to \infty$

Georges, Kotliar (1992)
mapping onto impurity problem,
self-consistent equations

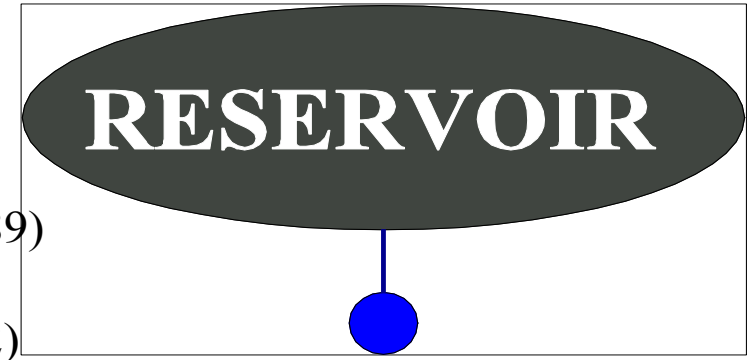

Effective impurity problem

$$\Sigma\left[\Delta(\omega)\right] = \Delta(\omega) - G^{-1}\left(\Delta(\omega)\right) + \omega \qquad G\left[\Delta(\omega)\right] = \sum_k \left\{\omega - \Sigma\left[\Delta(\omega)\right] - t_k\right\}$$

$$\Delta(\omega) = \sum_k \frac{\left|V_k\right|^2}{\omega - \varepsilon_k}$$

Dynamical Mean-Field Theory

Approximation: electron self-energy is local and does not depend on momentum (wave vector) ***k*** but only on frequency $i\omega_n$:

$$\Sigma(\mathbf{k}, i\omega_n) = \Sigma(i\omega_n)$$

Lattice Green function is defined by self-energy:

$$g_{ii}(i\omega_n) \equiv G(i\omega_n) = \sum_{\mathbf{k}} (i\omega_n + \mu - \epsilon_{\mathbf{k}} - \Sigma(i\omega_n))^{-1}$$

Hybridization of the site orbitals with the rest of the crystal in effective single impurity model is described by hybridization function $\Delta(i\omega_n)$ or non-interacting *bath* Green function $G_0(i\omega_n)$:

$$\mathcal{G}_0(i\omega_n) = (i\omega_n + \mu - \Delta(i\omega_n))^{-1}$$

Dynamical Mean-Field Theory

The DMFT mapping means:

$$G(i\omega_n) = G_{imp}(i\omega_n)$$
$$\Sigma(i\omega_n) = \Sigma_{imp}(i\omega_n)$$

Dyson equation for impurity problem:

$$G^{-1}_{imp}(i\omega_n) = \mathcal{G}_0^{-1}(i\omega_n) - \Sigma_{imp}(i\omega_n)$$

Dyson equation is used twice in DMFT. First for known self-energy and lattice Green function *bath* Green function is calculated:

$$\mathcal{G}_0^{-1}(i\omega_n) = G^{-1}(i\omega_n) + \Sigma(i\omega_n)$$

Then after impurity problem solution new approximation for self-energy can be defined:

$$\Sigma_{imp}(i\omega_n) = \mathcal{G}_0^{-1}(i\omega_n) - G^{-1}_{imp}(i\omega_n)$$

DFT+DMFT calculations scheme

Local Green function:

$$G^{loc}_{n,n'}(\varepsilon) = \frac{1}{V_{IBZ}} \int_{IBZ} d\mathbf{k} \left(\left[(\varepsilon + E_f^{(N)}) 1 - H_0^{WF}(\mathbf{k}) - \Sigma(\varepsilon) \right]^{-1} \right)_{n,n'}$$

Dyson equation defines bath Green function:

$$\mathcal{G}^{-1} = (G^{loc})^{-1} + \Sigma$$

Self-consistent condition:

$$G^{loc} = G^{imp} \Rightarrow \Sigma_{new}$$

Impurity problem defined by bath Green function is solved by QMC

DMFT calculations scheme

Impurity solvers:

- Quantum Monte Carlo method (QMC) – exact and efficient but very computer time consuming
- Numerical renormalization group (NRG) – unpractical for orbital degeneracy > 2
- Exact diagonalization method (ED) – discrete spectra and not suitable for orbital degenerate problem
- Iterative Perturbation Theory (IPT) – interpolation approximation
- Non-crossing Approximation (NCA)- first terms of hybridization expansion series

DMFT calculations scheme

Quantum Monte Carlo method (QMC)

discrete Hubbard-Stratonovich transformation:

$$H_{int} = U n_\uparrow n_\downarrow$$

Product $n_\uparrow n_\downarrow$ can be rewritten as a sum of quadratic and linear terms:

$$n_\uparrow n_\downarrow = -\frac{1}{2}(n_\uparrow - n_\downarrow)^2 + \frac{1}{2}(n_\uparrow + n_\downarrow)$$

Evolution operator $e^{\Delta\tau H_{\text{int}}}$ can be linearized by

$$e^{-\Delta\tau U n_\uparrow n_\downarrow + (\Delta\tau U/2)(n_\downarrow + n_\downarrow)} = \frac{1}{2}\sum_{s=\pm 1} e^{\lambda s(n_\uparrow - n_\downarrow)}$$

DMFT calculations scheme

Quantum Monte Carlo method (QMC)

where parameter : $\lambda = \operatorname{arccosh}\ (e^{\Delta\tau U/2})$

discrete field *s* is an Ising-like variable taking the values +1 and -1

Partition function $Z = \mathrm{Tr}\ e^{-\beta\mathscr{H}} = \mathrm{Tr} \prod_{l=1}^{L} e^{-\Delta\tau[\mathscr{H}^0 + \mathscr{H}^i]}$

the imaginary time interval is discretized into *L* time slices:

$\tau_l = l\Delta\tau \qquad l = 1,\ldots,L \ \text{ and } \ \Delta\tau \equiv \beta/L$

DMFT calculations scheme

Quantum Monte Carlo method (QMC)

$$Z \simeq Z^{\Delta\tau} \equiv \mathrm{Tr} \prod_{l=1}^{L} e^{-\Delta\tau \mathscr{H}^0} e^{-\Delta\tau \mathscr{H}^i}$$

Using Hubbard-Stratonovich transformation:

$$\exp[-\Delta\tau \mathscr{H}^i] = \frac{1}{2} \sum_{s=\pm 1} \exp[\lambda s (n_{d\uparrow} - n_{d\downarrow})]$$

and partition function becomes a sum over Ising fields s_l :

$$Z^{\Delta\tau} = \frac{1}{2^L} \sum_{s_1,\ldots,s_L=\pm 1} Z^{\Delta\tau}_{s_1,\ldots,s_L}$$

DMFT calculations scheme

Quantum Monte Carlo method (QMC)

$$Z^{\Delta\tau}_{s_1,\ldots,s_L} = \prod_{\sigma=\pm 1(=\uparrow,\downarrow)} \mathrm{Tr} e^{-\Delta\tau\mathscr{H}^0} e^{V^\sigma(s_1)} \times e^{-\Delta\tau\mathscr{H}^0} e^{V^\sigma(s_2)} \cdots e^{-\Delta\tau\mathscr{H}^0} e^{V^\sigma(s_L)}$$

$$e^{V^\sigma(s)} = \begin{pmatrix} e^{\lambda\sigma s} & \ldots & \ldots & 0 \\ \ldots & 1 & \ldots & \ldots \\ \ldots & \ldots & 1 & \ldots \\ 0 & \ldots & \ldots & 1 \end{pmatrix}$$

DMFT calculations scheme

Quantum Monte Carlo method (QMC)

$$G^{-1}_{\sigma,(s_1,\ldots,s_L)}(\tau,\tau') \equiv \mathcal{G}^{-1}_{0\sigma}(\tau,\tau')e^{V} + e^{V} - 1$$

$$Z = \sum_{\{s_1,\ldots,s_L\}} \det[G^{-1}_{\uparrow}(s_1,\ldots,s_L)]\det[G^{-1}_{\downarrow}(s_1,\ldots,s_L)]$$

$$G_\sigma = \frac{1}{Z} \sum_{\{s_1,\ldots,s_L\}} \det[G^{-1}_{\uparrow}(s_1,\ldots,s_L)] \times \det[G^{-1}_{\downarrow}(s_1,\ldots,s_L)] G_\sigma(s_1,\ldots,s_L)$$

DMFT calculations scheme

Quantum Monte Carlo method (QMC)

the total number of all possible spin configurations $\{s_j\} = s_1, \ldots, s_L$ for which one should calculate $G(\tau)$ is equal to 2^L ($\approx 2^{100} \approx 10^{30}$).
Many-dimensional integrals can be calculated by statistical Monte Carlo method.

$$\int d\mathbf{x} F(\mathbf{x}) P(\mathbf{x}) = \langle F \rangle \approx \sum_{\mathbf{x}_i} F(\mathbf{x}_i) P(\mathbf{x}_i) / \sum_{\mathbf{x}_i} P(\mathbf{x}_i)$$

Stochastically generated points in many-dimensional space x_i are accepted to be included in summation with probability proportional to

$$P(\mathbf{x}_i) \text{ and } \langle F \rangle = \sum_{\mathbf{x}_i} F(\mathbf{x}_i)/N_i$$

DMFT calculations scheme

Quantum Monte Carlo method (QMC)

probability *P* is proportional to

$$[detg^{-1\uparrow}_{s_1,\ldots,s_L} \cdot detg^{-1\downarrow}_{s_1,\ldots,s_L}]$$

physical Greens function is then given as an average of

$$g^{\sigma}_{s_1,\ldots,s_L}(\tau_l, \tau_{l'})$$

Probability of acceptance *P{s}→{s'}* for new configuration *{s'}* obtained from *{s}* is calculated according to Metropolis formula:

$$P_{\{s\}\to\{s'\}} = \begin{cases} 1 & \text{if } \frac{det(g')^{-1}}{detg^{-1}} > 1 \\ \frac{det(g')^{-1}}{detg^{-1}} & \text{in other case.} \end{cases}$$

DMFT calculations scheme

Quantum Monte Carlo method (QMC)

The Markov process is realized by going from configuration s to configuration s' by a single spin flip $s_p = -s_p$ with probability of acceptance $P\{s\}\rightarrow\{s'\}$ for new configuration $\{s'\}$ obtained from $\{s\}$
Markov chain is given by every accepted configuration:

$$\{s\} \rightarrow \{s'\} \rightarrow \{s''\} \rightarrow \{s'''\} \rightarrow \dots$$

instead of summation with weights $Zs_1,\dots,s_L$ an averaging of $g^{\sigma}_{s1,\dots,sL}(\tau_l, \tau_{l'})$ over all accepted configuration is performed because probability of acceptance is proportional to $Zs_1,\dots,s_L$.
Number of Markov chain "sweeps" is usually $\approx 10^6$ that is much smaller then total configurations number 2^L $(\approx 2^{100} \approx 10^{30})$.

DMFT calculations scheme

Total energy calculation in LDA + DMFT

$$E_{tot} = E_{LDA} + E_{DMFT} - E_{MF} \ ,$$

where E_{LDA} is total energy obtained in *LDA* calculation, E_{DMFT} is an energy calculated in *DMFT* and E_{MF} is an energy corresponding to static mean-field approximation (restricted Hartree-Fock) for the same Hamiltonian as used in *DMFT* calculations.

$$E_{DMFT} = \frac{1}{\beta}\frac{1}{V_B}\int \mathrm{d}\mathbf{k} \sum_n Tr\hat{H}_0(\mathbf{k})\hat{G}_{\mathbf{k}}(i\omega_n)e^{i\omega_n 0^+} +$$

$$+ \frac{1}{2}\sum_{i=i_d,l=l_d}\sum_{m,m',\sigma}\{U_{mm'}\langle\hat{n}_{ilm\sigma}\hat{n}_{ilm'\bar{\sigma}}\rangle + (U_{mm'} - J_{mm'})\langle\hat{n}_{ilm\sigma}\hat{n}_{ilm'\sigma}\rangle\}$$

DMFT calculations scheme

Total energy calculation in LDA + DMFT

where $G_k(i\omega_n)$ is electronic Green function corresponding to wave vector k

$$\hat{G}_{\mathbf{k}}(i\omega_n) = \left[(i\omega_n + \mu)\hat{I} - \hat{H}_0(\mathbf{k}) - \hat{\Sigma}(i\omega_n)\right]^{-1} ,$$

The average values for particle number operators products $\langle n_{ilm\sigma}\, n_{ilm'\sigma}\rangle$ can be calculated directly in QMC method

Energy corresponding to static mean-filed approximation E_{MF} is calculated analogously with replacing interacting Green function $G_k(i\omega_n)$ on $G^{LDA}_k(i\omega_n)$ calculated with LDA Hamiltonian:

$$\hat{G}^{LDA}_{\mathbf{k}}(i\omega_n) = \left[(i\omega_n + \mu)\hat{I} - \hat{H}^{LDA}(\mathbf{k})\right]^{-1} ,$$

DMFT calculations scheme

Total energy calculation in LDA + DMFT

and also with replacing second term in E_{DMFT} on Coulomb interaction energy in the following form:

$$E_{Coulomb} = \sum_{i=i_d, l=l_d} \frac{1}{2} \bar{U} n_d (n_d - 1)$$

where n_d is a total correlated electrons number on the site i_d
and U is an average value of Coulomb interaction between different orbitals.

DMFT calculations scheme

Maximum entropy method for analytical continuation on real energies

QMC calculation procedure results in Matsubara Green function $G(\tau)$ for discrete imaginary time points $\tau_l - \tau_{l'}$ or imaginary energies $G(i\omega_n)$. Spectral function $A(\omega)$ for real energies ω is solution of integral equation:

$$G(\tau) = -\int_{-\infty}^{\infty} d\omega \frac{e^{-\tau\omega}}{1+e^{-\beta\omega}} A(\omega)$$

Entropy maximization principle accounts for stochastic noise in QMC Green function

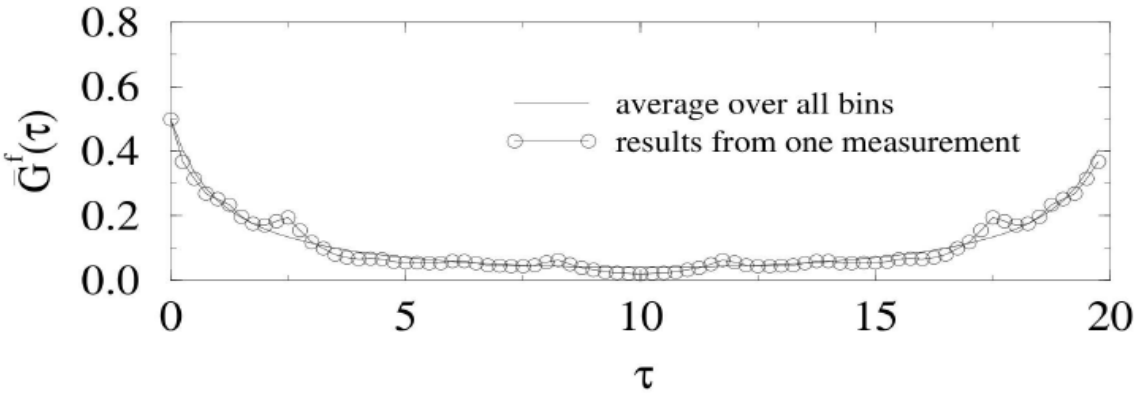

DFT+DMFT calculations scheme

Calculation scheme of

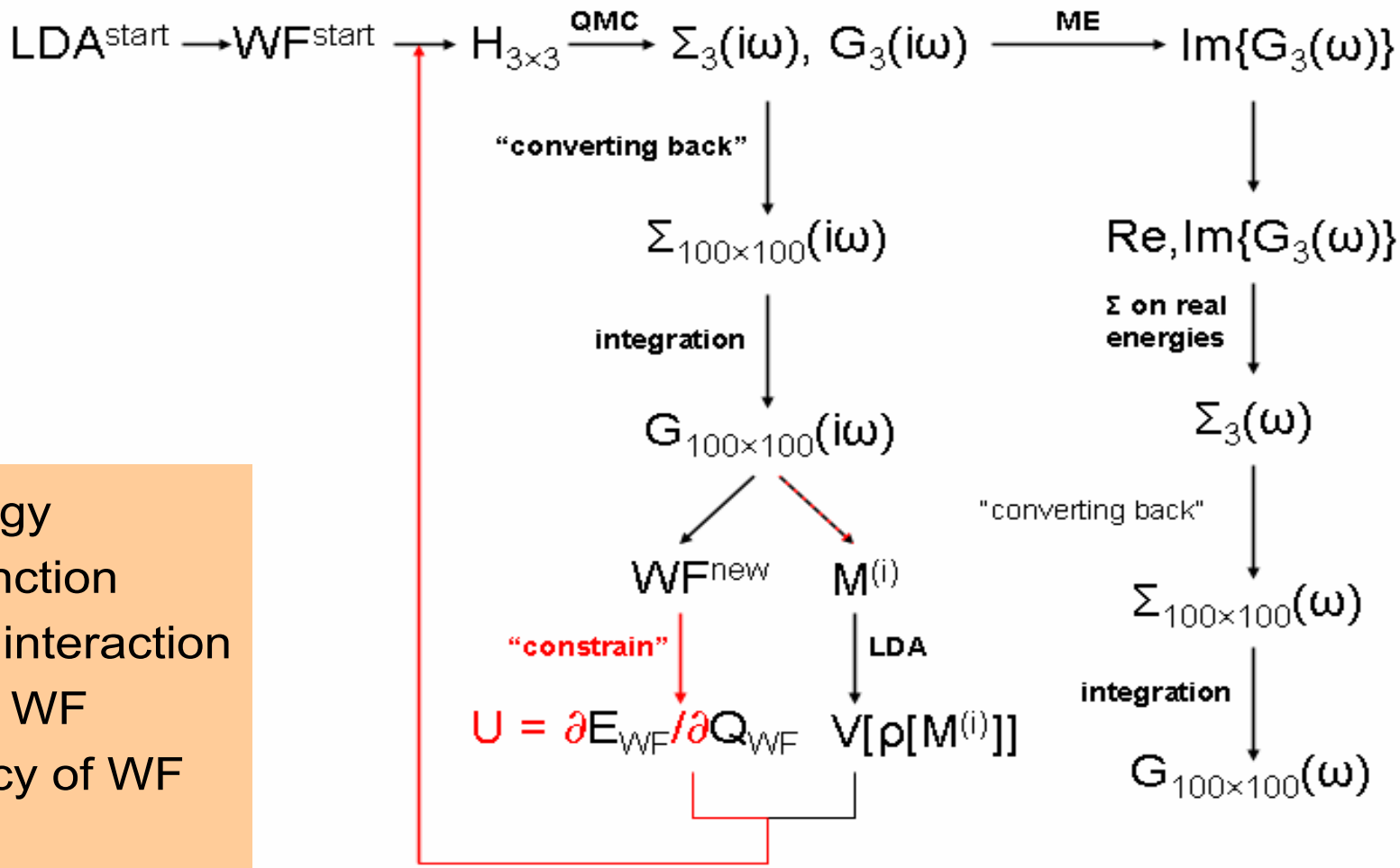

Σ – Self-energy
G – Green function
U – Coulomb interaction
$\mathbf{E_{WF}}$ – Energy of WF
$\mathbf{Q_{WF}}$ – Occupancy of WF
$\mathbf{M^{(i)}}$ – Moments
V – DFT potential

V.Anisimov et al, Phys. Rev. B 71, 125119 (2005).

Dynamical Mean-Field Theory

Spectral function and self-energy

$$G(\varepsilon) = \sum_k (\varepsilon - \varepsilon(k) + i\eta)^{-1} \qquad G(\varepsilon) = \sum_k (\varepsilon - \varepsilon(k) - \Sigma(\varepsilon))^{-1}$$

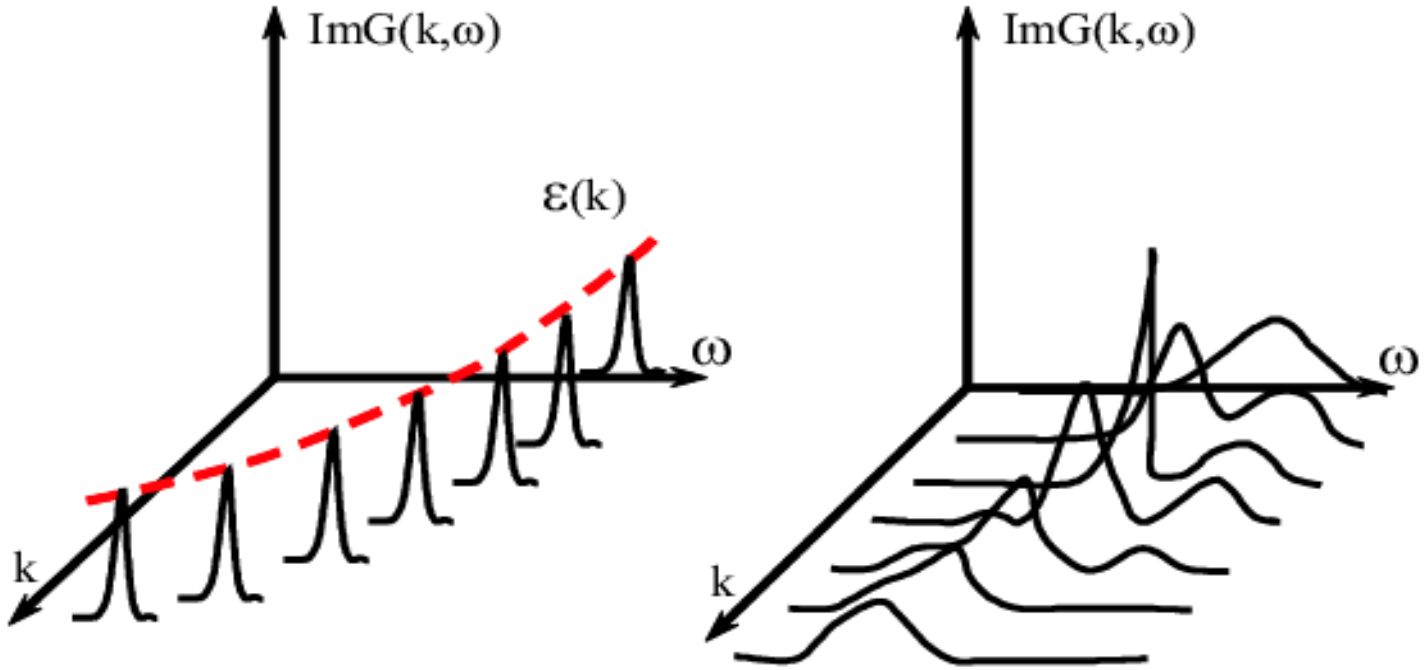

Dynamical Mean-Field Theory

Three peak spectral function and metal insulator transition in DMFT

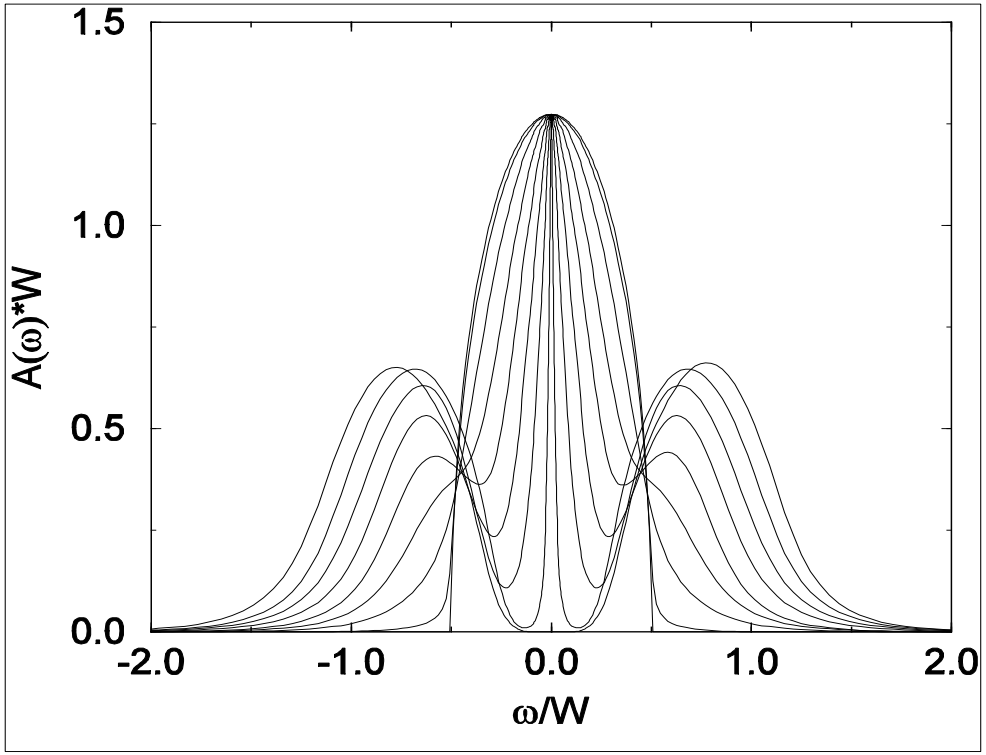

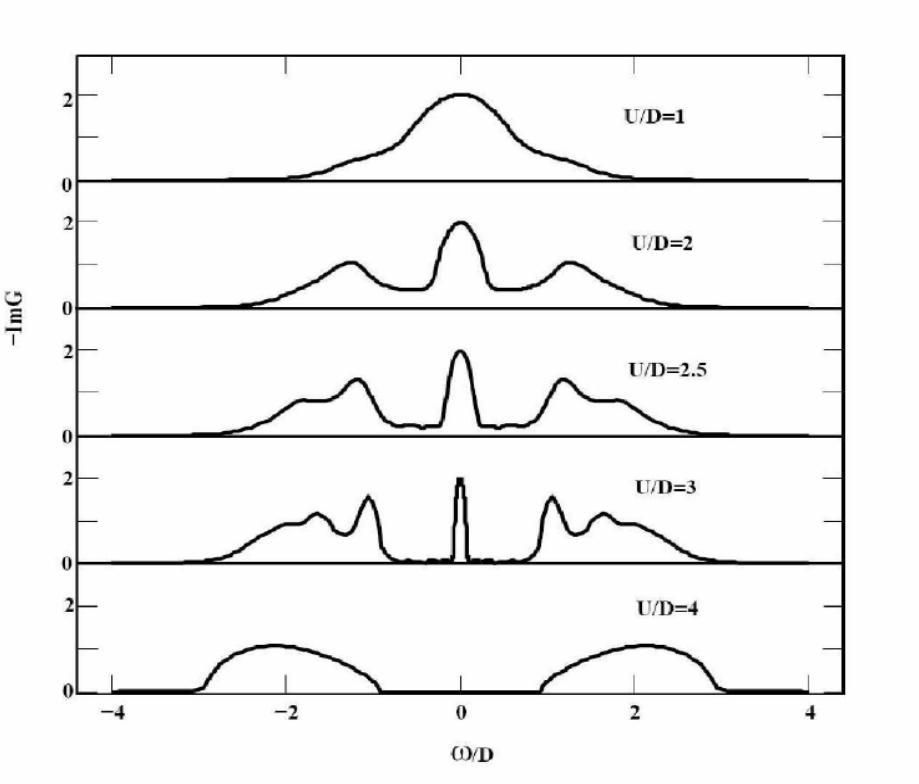

A. Georges et al, Rev. Mod. Phys 68, 13 (1996)

Dynamical Mean-Field Theory

Three peak spectral function and metal insulator transition in DMFT

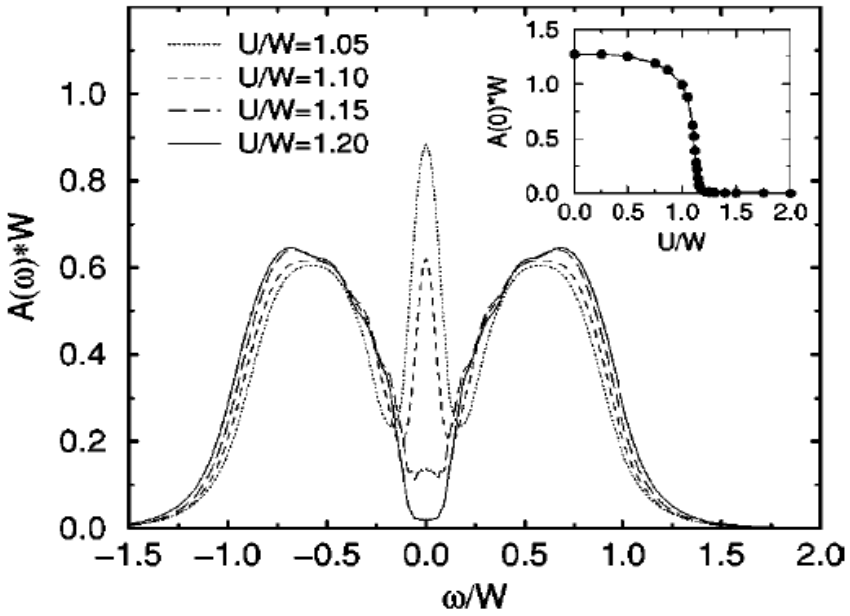

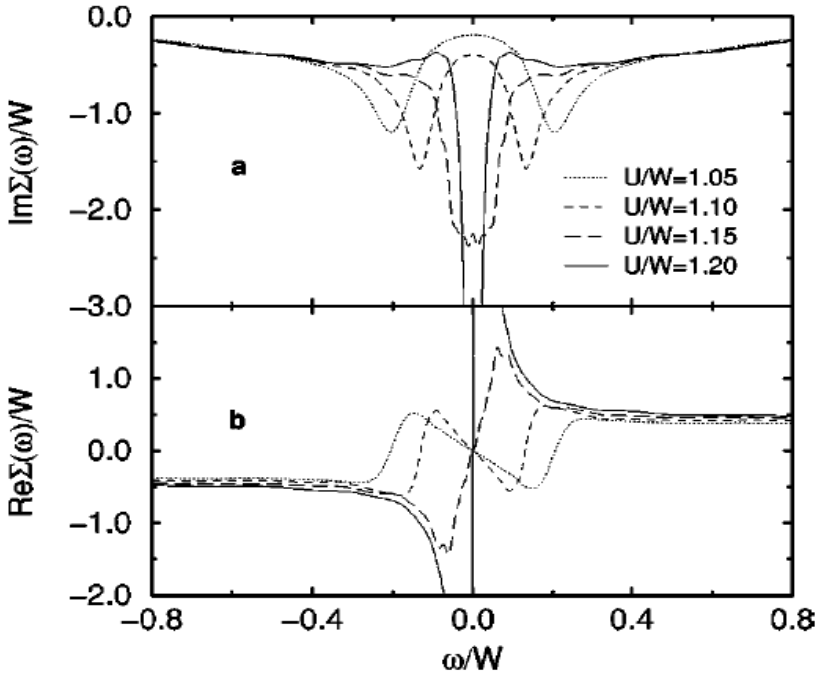

R. Bulla et al, Phys. Rev. B 64, 045103 (2001)

Dynamical Mean-Field Theory

Temperature dependence of quasiparticle peak in DMFT

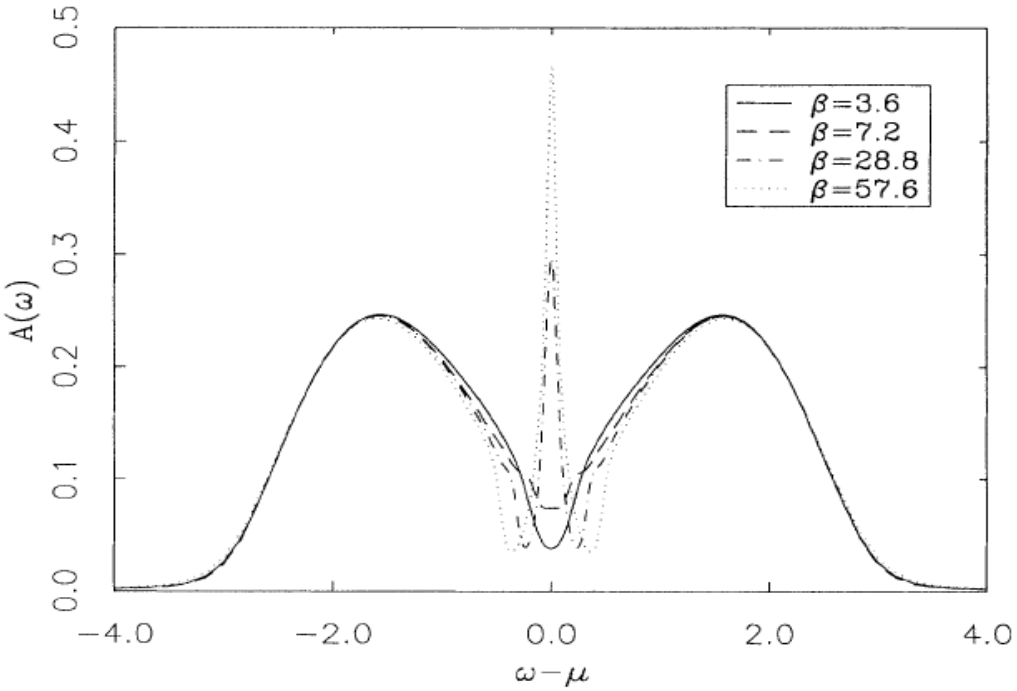

Half-filling

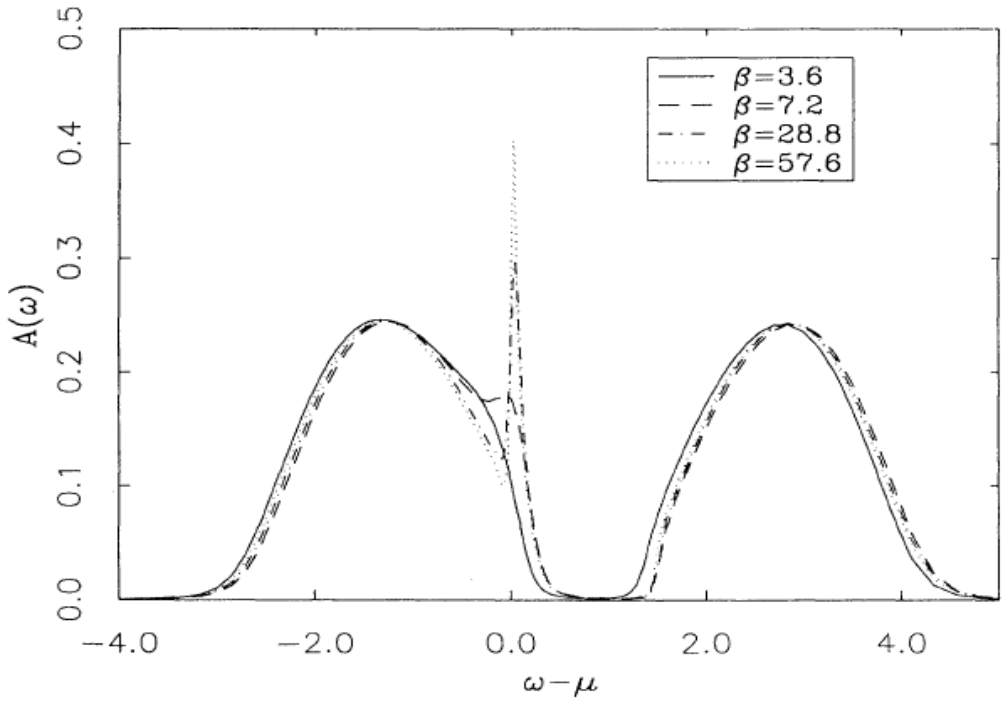

0.03 hole doping

Th. Pruschke et al, Phys. Rev. B 47, 3553 (1993)

Dynamical Mean-Field Theory

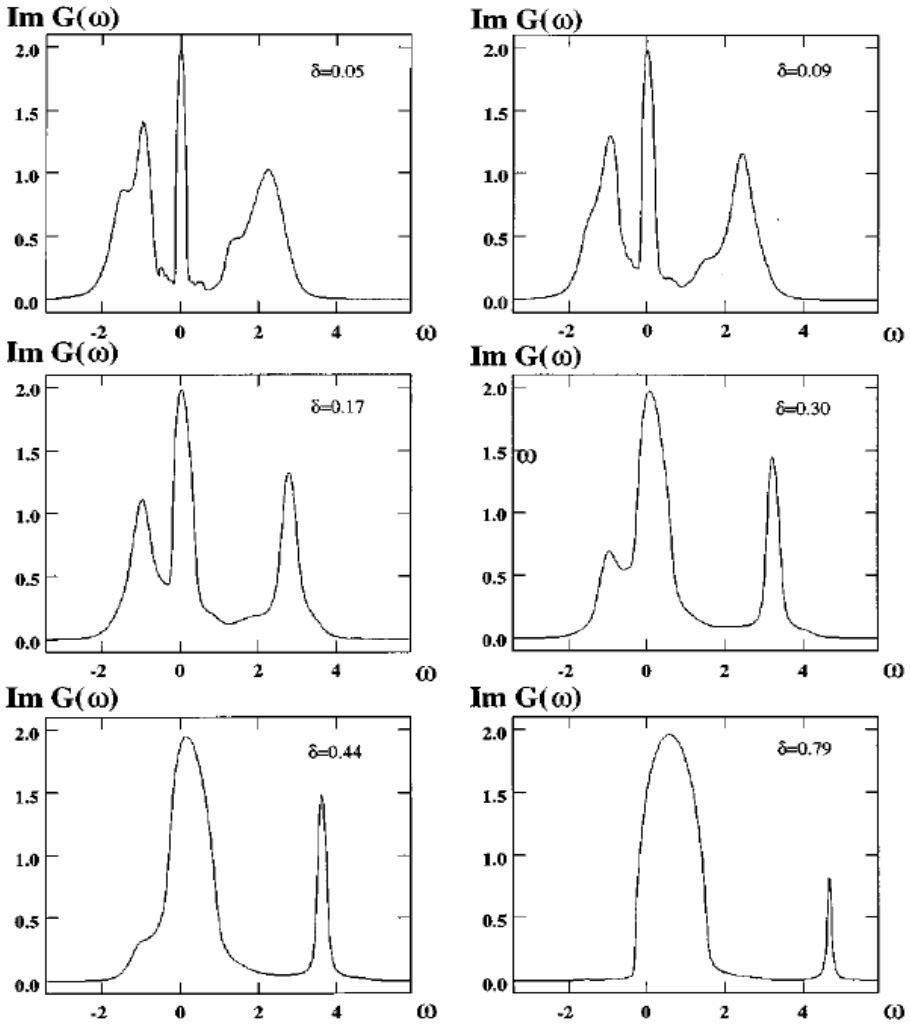

Suppression of correlation strength and spectral weight transfer between Hubbard bands with hole doping in non-degenerate Hubbard model

H. Kajueter et al, Phys. Rev. B 53, 16 214 (1996)

Dynamical Mean-Field Theory

Orbital degeneracy dependence of quasiparticle peak in DMFT

Half-filling

n=0.9

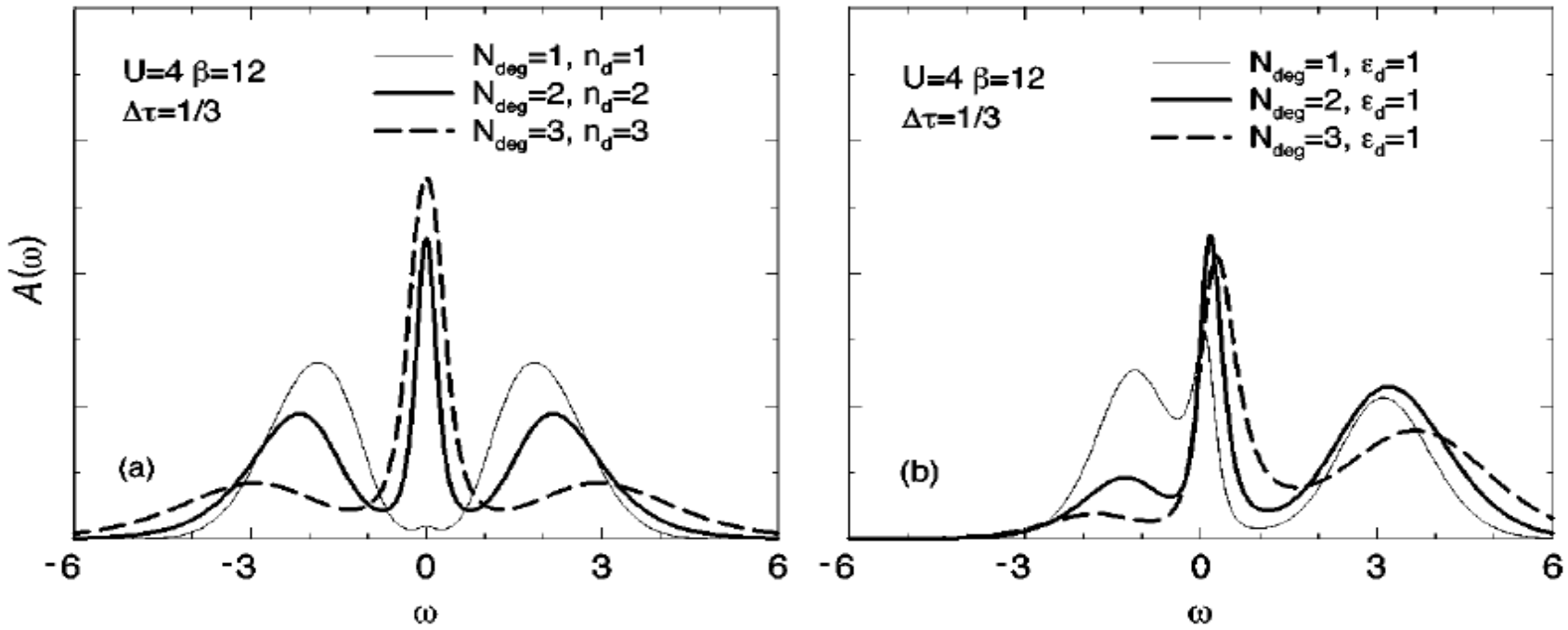

$$U_c(N_{\mathrm{deg}},J) \approx \sqrt{N_{\mathrm{deg}}}\,U_c(1,0) - N_{\mathrm{deg}}J$$

J. E. Han et al, Phys. Rev. B 58, R4199 (1998)

Dynamical Mean-Field Theory

Orbital degeneracy dependence of quasiparticle peak in DMFT

Triply degenerate band

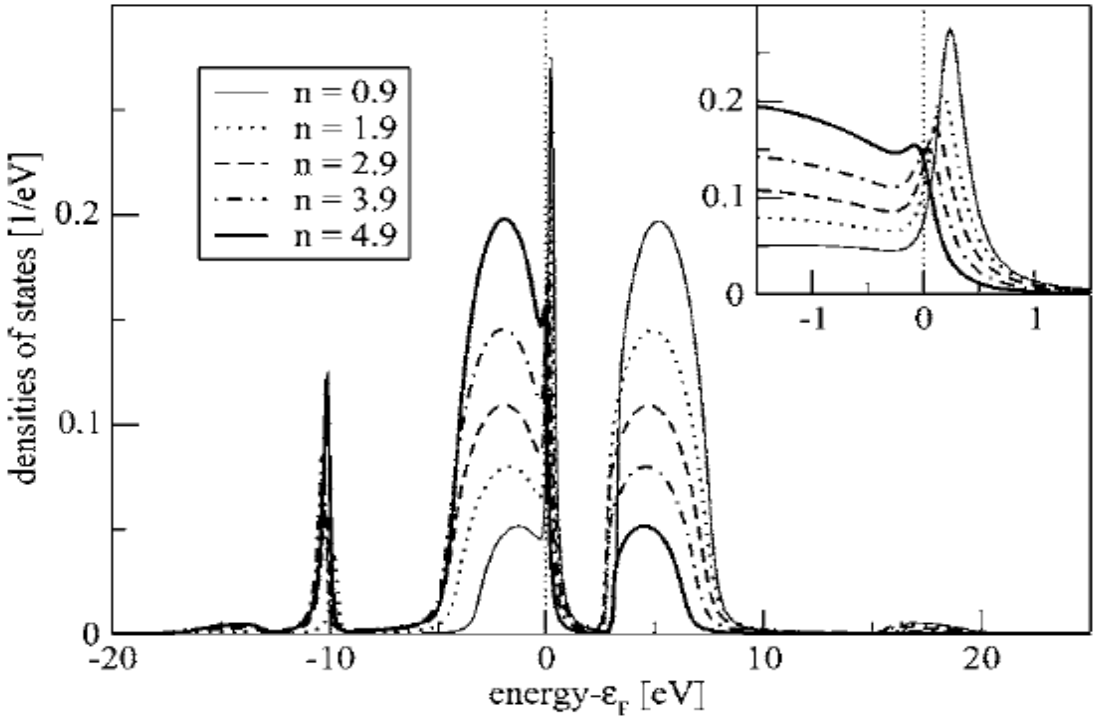

P. Lombardo et al, Phys. Rev. B 72, 245115 (2005)